

A Review on Segmented Switched Reluctance Motors

Zhenyao Xu ^{1,*} , Tao Li ¹, Fengge Zhang ¹, Yue Zhang ², Dong-Hee Lee ³ and Jin-Woo Ahn ³¹ School of Electrical Engineering, Shenyang University of Technology, Shenyang 110870, China² School of Electrical Engineering, Shandong University, Jinan 250061, China³ Department of Mechatronics Engineering, Kyungsoong University, Busan 48434, Republic of Korea

* Correspondence: xuzu@sut.edu.cn; Tel.: +86-24-25496520

Abstract: The switched reluctance motor (SRM) benefits from its magnet-free nature, robust construction, low cost, flexible controls, and the ability to operate in harsh environments such as high temperatures and high pressure. It has received increasing attention for all-electric or multi-electric aircraft systems and electric vehicles (EVs) as compared with permanent magnet synchronous motors (PMSM) and other AC motors in some required high reliability and fault tolerance applications. However, the SRM is prone to considerable wind resistance due to the convex pole structure of the rotor during high-speed rotation, high torque ripple, and also vibration noise. Thus, it is currently a trending topic to develop special SRMs, tailored with high reliability and fault tolerance. Recent research demonstrates several promising feasible solutions to reduce torque ripples and enhance torque density and power factors, including changing topology of SRM, using advanced control methods, as well as different winding configurations. Among these options, the segmented switched reluctance motor (SSRM), as a deformation of the conventional topology, is shown to be capable of effectively optimizing the torque performance. Motivated by this advance, this paper aims to present a comprehensive literature review on the SSRM, first illustrating the development of the topology of the SRM, then providing a description as well as a classification according to the topology of the SSRM. In particular, we focus on the evolution of various kinds of segmental topology and improvement measures. Then, we discuss the performance, advantages, and disadvantages of various types of structures in terms of their electromagnetic aspects and their applications. Eventually, several promising future trends and application prospects of the SSRM are prospected, with the aim of shedding light on further research. In sum, the key contribution of this paper is to provide a valuable basis for detailed analyses of the structure and electromagnetic design of the SSRM that are expected to benefit future research.

Keywords: switched reluctance motors; segmental rotor; segmental stator; high torque density

Citation: Xu, Z.; Li, T.; Zhang, F.; Zhang, Y.; Lee, D.-H.; Ahn, J.-W. A Review on Segmented Switched Reluctance Motors. *Energies* **2022**, *15*, 9212. <https://doi.org/10.3390/en15239212>

Academic Editor: Adolfo Dannier

Received: 10 November 2022

Accepted: 30 November 2022

Published: 5 December 2022

Publisher's Note: MDPI stays neutral with regard to jurisdictional claims in published maps and institutional affiliations.



Copyright: © 2022 by the authors. Licensee MDPI, Basel, Switzerland. This article is an open access article distributed under the terms and conditions of the Creative Commons Attribution (CC BY) license (<https://creativecommons.org/licenses/by/4.0/>).

1. Introduction

With the rapid development of power electronics and the gradual increase in the cost of permanent magnets (PMs), the switched reluctance motor (SRM) has been widely used in critical applications, such as starter/generators for aviation [1], driving systems for electric or hybrid vehicles [2–4], and household appliances [5], owing to its special and elaborated structure. Although SRM has lots of merits over induction motors (IM) and permanent magnet synchronous motors (PMSM), its shortcomings of noise, low power density, and radial vibration cannot be ignored. In an ideal SRM, the reluctance varies linearly with stator teeth overlap, generating a constant torque for a constant magnetic motive force (MMF). It is always designed to operate within the magnetic saturation zone of the ferromagnetic material to maximize torque density. However, in practical terms, saturation, magnetic field edge flux, and the rotor's biconvex pole structure make the constant phase current produce torque and flux as a nonlinear function of rotor position. As a result, the generated torque may contain significant torque fluctuations, while torque ripple is believed to contribute significantly to another shortcoming of SRM, acoustic noise.

In the last few years, the research on the structure of SRMs has focused on segmental, bearingless, and linear types, from the traditional long flux path to the novelty short flux path, as shown Figure 1. In some industrial applications that require high-speed rotation, conventional switched reluctance motors (CSRMs) typically adopt mechanical bearings to support the shaft of the motor system, causes severe wear on the mechanical bearing under long-term operation and leads to more heating problems. In severe cases, it will affect the uniformity of the air gap between the stator and rotor. It not only affects the efficiency of the motor, but also shortens the useful life of the machine and increases the maintenance burden of the motor and bearings. Moreover, the lubricant required for the mechanical bearings cannot be used in harsh environments such as vacuums and high temperatures. In order to solve the various problems posed by mechanical bearings in high-speed SRMs, air float, liquid float, and magnetic levitation bearings emerged in the community. Although these measures can achieve contactlessness and frictionlessness between shaft and rotor, air float and liquid float technologies must be equipped with special pneumatic and hydraulic systems. However, it will also make the motor larger. When the air pressure or hydraulic system fails, the air float and liquid float bearing will also fail. Consequently, the motor cannot run normally, thereby reducing the reliability of the motor system. The magnetic bearing technology fundamentally changed the traditional support form, with no contact between the shaft and rotor, high speed, high precision, long life, and other characteristics. On this basis, the seminal work of Higuchi proposed the concept of bearingless switched reluctance motors (BSRMs). However, it was not until the late 1990s that a more systematic study of BSRMs was conducted. For example, in [6], Takemoto exploited the similarity between the stator structure of SRMs and magnetic bearings by superimposing the levitation force winding of magnetic bearings on the stator windings of SRMs, such that the motor generates both levitation force and electromagnetic torque to achieve levitation and rotation of the motor rotor, thereby discarding the conventional bearing and reducing the weight of the SRM.

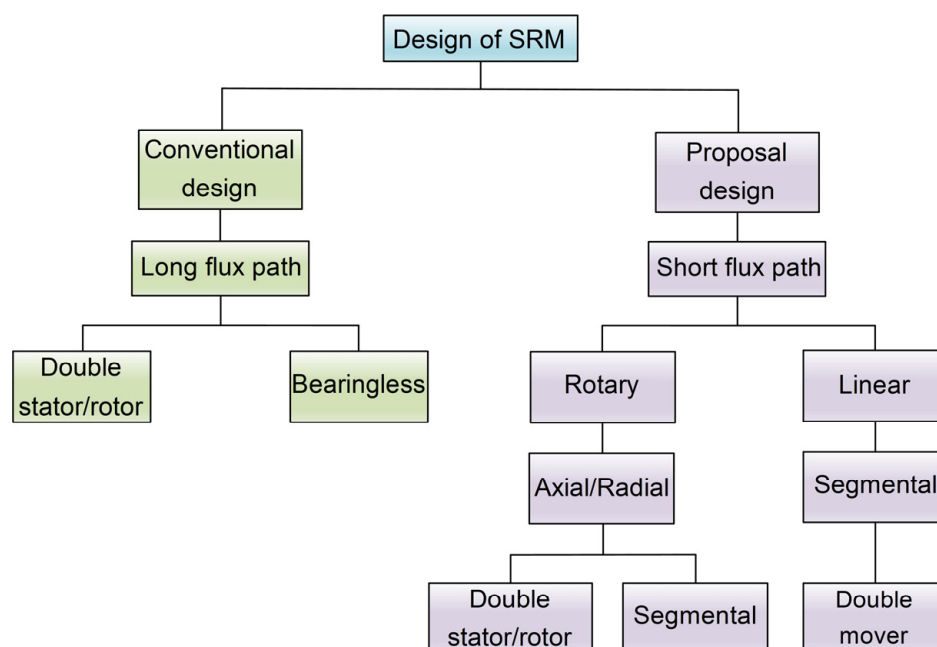


Figure 1. A classification of existing SRM topologies in recent years.

The segmental structure is a new topology based on the optimization of the flux path of the CSRMs, of which the basic idea is to convert the stator or rotor from the previous conventional continuous iron core structure into discontinuous segments embedded in an isolator made of non-magnetic material to form a special short flux path which will reduce the coupling of adjacent phase fluxes and core losses. This idea was pioneered

proposed by Lawerson, who divided the rotor of a synchronous reluctance motor (SynRM) into several discontinuous segments and replaced the magnetically conductive material in the center of the rotor with a non-magnetic material. It aims at increasing the magnetic utilization of SynRM by having more than half of the magnetic iron structure carry machine flux with short flux paths at any time during machine operation. Instead of the use of the conventional rotor teeth structure, it is constructed from a series of discrete segments. This method paved the way for the future research on the segmented switched reluctance motor (SSRM) [7].

To solve the problem of high wind resistance caused by the rotor convex pole structure when the SRM is running at a high speed, Morel and Hamdy proposed adding filler to the rotor slot [8] and adding a barrier between the adjacent rotor poles [9]. Experiments have shown that, although it can effectively reduce wind resistance, it will increase the motor machining process, which is unsuitable for practical industrial production and leads to safety impacts during high-speed rotation of the motor. At the beginning of the 21st century, some researchers gradually began conducting systematic research on the SSRM. The results of various studies have shown that the segmental structure can make better use of its special magnetic circuit path, thus providing greater electromagnetic torque and power density than the CSRSM with the traditional convex pole structure. Therefore, it has a wide range of development prospects in the field of aviation, textile machinery, drive systems for general industry and electric vehicles, as well as some other vital applications.

In this paper, we summarize the milestone research progress and the latest research advance on the topology of the SSRM in recent years, followed by a detailed analysis of the development trend of the structural design. In particular, we include the state-of-the-art methods of the segmental rotor, segmental stator, and other new types of SSRM, and discuss the essential characteristics of each structure and compare their relative merits and limitations. Then, we demonstrate the promising applications with these approaches. Furthermore, we also provide a discussion on the basic methods of the electromagnetic design of segmented structures. Finally, the development trend and research direction of SSRMs are summarized for future research.

2. Conventional Segmental SRM

2.1. Segmental Rotor Type

2.1.1. Structure of Segmental Rotor Type

An electromagnetic design alternative to the CSRSM was firstly proposed and studied in detail by Mecrow. A new type of three-phase 12/8 segmental rotor SRM was fabricated and tested in [10–12]. The topology and the flux path distribution of phase A are shown in Figure 2. The stator and rotor prototype are presented in Figure 2b,c. The rotor segments consist of a series of discrete laminated sheets. Eight identical fan-shaped rotor segments are mounted directly on a non-magnetic isolator made of metallic aluminum and then encapsulated with epoxy resin after assembly. The flux path is shorter than that of the CSRSM and only passes through two adjacent stator tooth poles and rotor segment closures, with each coil linking two stator teeth with magnetic flux. Hence, the magnetic flux-linkage value in the aligned position is nearly twice that of the CSRSM as shown in Figure 3, which improved the rate of electromagnetic utilizations. However, the minimum flux-linkage at the unaligned position is about three times that of the conventional structure. The stator winding of the 12/8 segmental rotor SRM is connected by the full-pitch windings (FPW), and each phase winding needs to be closed across three stator teeth. Experiments show that the torque of the new structure is nearly 40% higher than the traditional structure SRM, but the copper loss per unit of torque is increased by 14%. There are also some other challenges, such as weaker mechanical strength and complicated manufacturing. The flux reversal will occur in stator teeth during the phase changed, which increases the stator core loss.

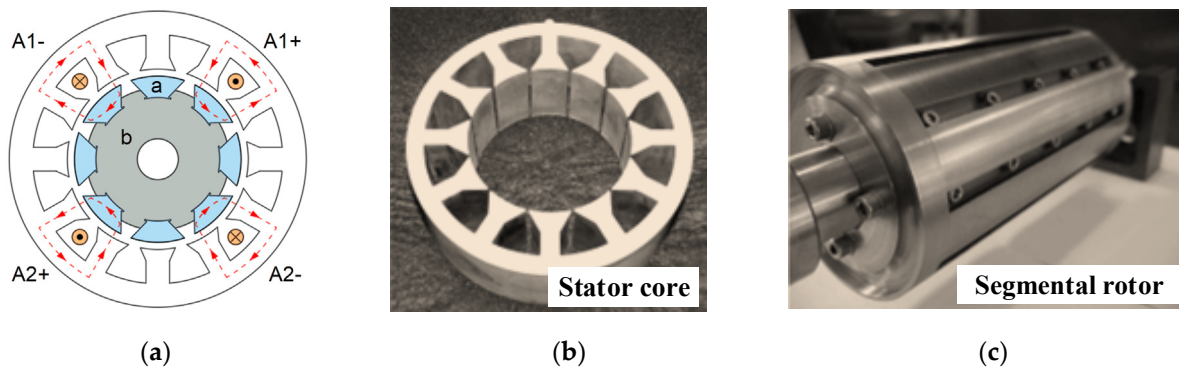


Figure 2. Proposed 12/8 segmental rotor SRM with FPW. (a) is the topology of proposed SSRM where “a” is the segmental rotor and “b” is the rotor block; (b,c) is the stator and rotor core.

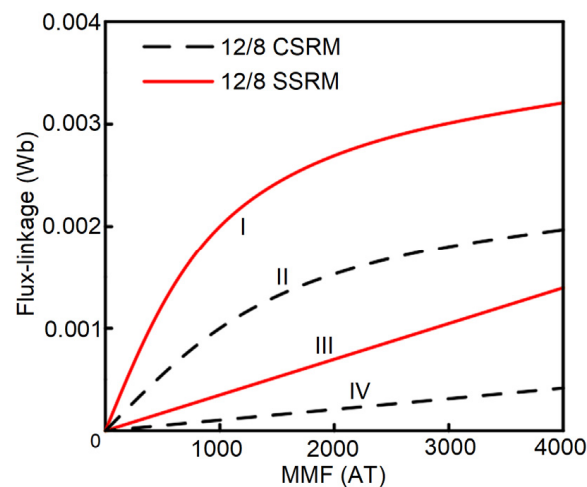


Figure 3. The Flux/MMF characteristics comparison. Notes: “I” and “II” is the aligned position’s curve; “III” and “IV” is the unaligned position’s curve between 12/8 CSRMs and segmental rotor SRM.

In response to these problems, Oyama extended this concept by improving the manufacturing process on the rotor, with the rotor segments embedded directly in a solid aluminum rotor block used in a three-phase 6/4 SSRM. Unfortunately, however, the mechanism of attachment is not explained [13,14]. As shown in Figure 4a, this structure improves the mechanical strength and is easier to manufacture. The optimal turn-on and turn-off angles of the motor were determined by finite element analysis. The 6/4 segment structure improved the electromagnetic torque compared to the conventional structure, reducing the single tooth radial force by 76% and significantly reducing vibration. However, the torque ripple was not well suppressed. The FPW still connect the stator’s winding, and the two radially opposite teeth are connected in series to form one phase. Oyama built and tested this machine and was able to develop a substantial body of performance evidence. Of most interest is the assessment that the efficiency and power factor of this type of segmental rotor SRM would be reduced compared to a CSRMs at higher output powers. Both Mecrow and Oyama demonstrate that, in these machines, flux is linked round a single slot, implying that a constant width flux path encompassing rotor segments, stator teeth, and stator core back iron may potentially be the optimum design solution. If this methodology were followed, it may be possible to increase the slot area, allowing for the use of lower resistance windings and decreasing copper loss. However, it is possible that the wider stator tooth becomes appropriate once more than one phase is conducting simultaneously as in actual operation, where each tooth may need to carry flux from more than one coil. A further concern with Oyama’s design is that the aluminum rotor support impinges into close proximity with the air gap. This could be expected to result in significant eddy current losses in the support,

where the support itself should not be laminated. To further optimize the performance of the 6/4 segmental rotor SRM, the motor was improved by increasing the number of motor phases, changing the rotor segment structure, and using rotor segments made of particular grain-oriented electrical steel [15–17]. Higuchi reviewed the performance of four-phase, five-phase and six-phase SSRMs and concluded that the four-phase motor achieved the best performance in reducing torque ripple, and also observed that this configuration improved the motor's torque density [15]. However, the complexity and cost of a four-phase drive will be higher than that of an equivalent three-phase drive. The stepped segmental rotor section structure is shown in Figure 4c, including a 7° skew in the rotor segment. Although the average torque is reduced by 10% compared to the original, the torque pulsation is reduced by 19%, and the vibration is reduced to 52%, with a significant vibration suppression effect due to the introduction of the rotor skew.

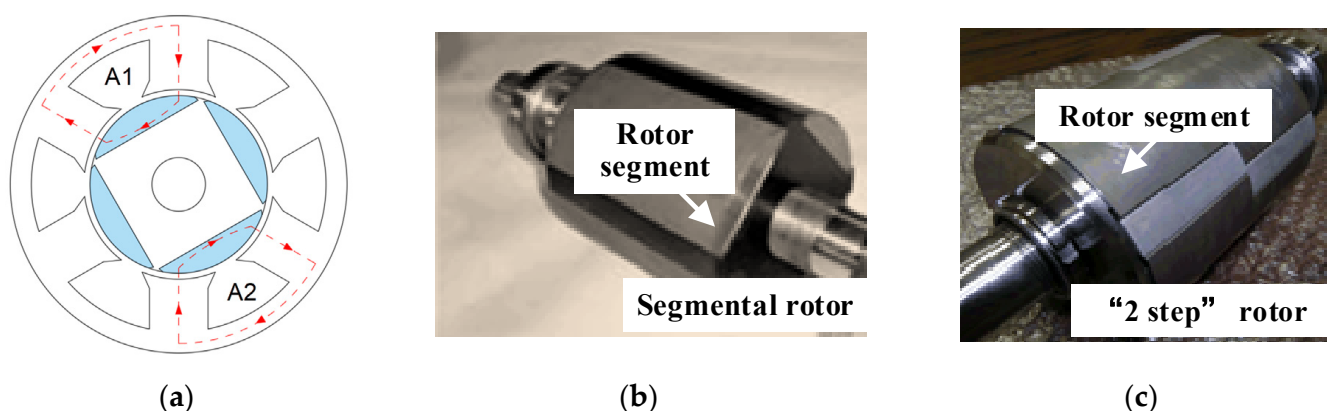


Figure 4. Proposed 6/4 SSRM with FPW. (a) is the topology of the proposed SSRM (the blue area is segmental rotor); (b,c) depict a segmental rotor and a “2-step” rotor, respectively.

Through further optimization of the motor's structure, Vandana designed a high torque, low weight circular slot segmental rotor SRM [18,19], shown in Figure 5a. The stator is wrapped in a layer of stator sleeves, the stator groove is circular, and the magnetic flux is forced to follow a circular path. The length is further shortened. The stator structure of its circular groove does not have a continuous stator yoke; it is instead connected by relatively independent stator segments, and the larger stator rotor polar arc increases the contact area of the air gap. As such, the magnetic flux at the aligned position also increases. The minimum inductance at the unaligned position is basically unchanged. The special flux path allows the motor to have no magnetic flux reversal when commutating, thereby reducing core loss. Compared with the 6/4 CSRSM, the weight is reduced by 14%, the slope of the inductance curve is increased, the torque is increased by 62%, and the torque density is further improved. The width of the constant inductance region is reduced, decreasing the torque ripple during the change of phase. The rotor segments are embedded directly in the non-magnetic isolator for mechanical stability and are suitable for aerospace, automotive, and military applications. However, it appears that the improvements underpinning assessment were flawed. Vandana's assessment was based on the torque performance of various machines for a given magnetic motive force. However, a review of his proposed design leads to the conclusion that the slot area would be significantly reduced in the region of 50% over Mecrow's design. This would lead to a significant increase in current density for fixed slot fill factors, and also result in a large increase in copper losses. It should also be noted that Vandana does not construct a prototype machine and the results have not been experimentally confirmed.

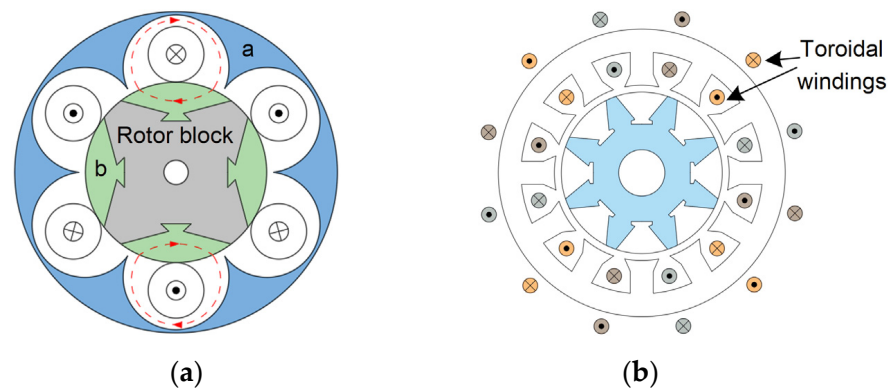


Figure 5. Proposed improvement measures for segmental rotor SRM. (a) is the circle stator slot topology for 6/4 segmental rotor SRM where “a” is the stator sleeve and “b” is the segmental rotors; (b) is the proposed toroidal winding connection.

The stator windings of a segmental rotor SRM with an FPW connection need to span “ m ” stator teeth, where m is the number of the phase of the motor. Each phase of winding overlaps at the end, making the motor’s end very large and also increasing the end effect of the motor, which literally improves the torque output capacity at the expense of increasing the length of the end winding, reduces the utilization rate of the winding and the reliability of the motor, and is not conducive to heat dissipation. Therefore, when performing finite element analysis, the 3D analysis method can be used. The calculation accuracy of phase inductance and torque is high due to consideration of the end effect and the leakage of the magnetic fields of other components [20]. Because of the problem of the long end of the FPW, some researchers have improved the connection method of the coil and proposed a connection method for the toroidal windings [21] as shown in Figure 5b. These windings are wound around the yoke of each stator slot. To prevent magnetic flux reversal in the stator tooth during commutation, the polarity of the adjacent phase windings must be reversed, and the entire winding resembles a toroidal winding. The use of this winding connection method makes the motor phase windings almost without overlapping at the end, thereby reducing the length of the end winding and increasing the utilization rate of the winding. In fact, however, the outer diameter of the motor is increased in the radial, and the winding is wound axially through the stator slot, which increases the difficulty of winding and is not suitable for actual industrial production.

Mecrow then proposed a concentrated winding (CW) type three-phase 12/10 segmental rotor SRM by optimizing the stator core structure [22]. All coils span only one stator tooth, the stator poles are divided into wide and narrow teeth, and windings are wound only on the wide teeth for generating the main flux. In contrast, the narrow teeth provide the path for the flux return only. The magnetic flux flows downward along the wide tooth and returns from the adjacent narrow tooth through the rotor segment. Thus, the magnetic flux carried by the wide teeth is approximately equal to the sum of the magnetic flux carried by the narrow tooth on both adjacent sides, provided that the phase magnetic leakage is ignored. The basic structure is shown in Figure 6, where the stator slot contains the coils of only one phase, wound at each interval of one stator tooth. The windings of each phase do not overlap at the ends and the windings is tiny compared with FPW, which improves the utilization of the windings, enhances the reliability of the motor, and makes the motor shorter and more compact. However, the space of the stator slot is reduced, which reduces the stator slot space area and limits further optimization of the motor. Compared to 12/8 CSRSM, the new structure offers a 44% improvement in torque performance with roughly the same winding losses per unit of torque, and at the same time inherits other advantages of the FPW segmental rotor SRM, such as the shorter flux path, wind resistance, lower weight, etc.

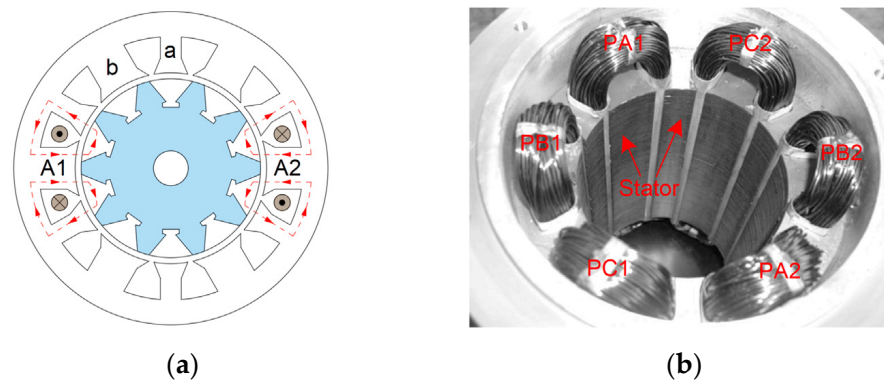


Figure 6. Proposed 12/10 segmental rotor SRM with CW. (a) is the radial model for motor where “a” is a narrow tooth and “b” is a wide tooth; (b) is the prototyped of motor’s windings and stator.

The switching frequency f_D of the SRM’s drive circuit can be expressed by (1), where N_r and n denote the number of rotor segments and rotation speed. It can be seen that, under the same speed, the higher the number of rotor segments, the higher the switching frequency that will be produced and the consequent switching losses. The frequency of change of the stator core flux also increases, which will increase the losses in the motor system. The increase in the number of phases or poles leads to an increase in motor and controller costs. Thus, motors with a large number of phases or poles are not suitable for high-speed drives.

$$f_D = (mN_r n) / 60 \quad (1)$$

Suppose the adverse effects of the increased number of rotor segments on motor losses, manufacturing costs, motor weight, and control difficulties are not considered. In that case, the segmental rotor SRM has better performance at low speeds and low current densities when the number of rotor segments is greater than stator poles [23]. The increasing number of rotor segments results in a larger magnetic co-energy per revolution of the motor, which leads to an increase in torque. However, this improvement is limited by the iron loss, and the higher the number of rotor segments, the higher iron loss will be produced, especially in high-speed operation.

Xu proposed three-phase 6/5 and 12/8 segmental rotor SRMs with CW for vehicle cooling fans [24–26]. The wide teeth were defined as excitation poles and the narrow teeth were defined as auxiliary poles. All conductors in each stator slot are coupled only to their own MMF-driven flux. The mutual coupling between adjacent phases is small, increasing the electrical utilization and reducing the MMF requirements of the motor, effectively improving the output torque compared with the conventional 12/8 SRM. The basic structures of the 6/5 and 12/8 segmental rotor SRM are shown in Figure 7a,b. The winding generated flux flows downward from the excitation pole, through the rotor segment, and returns from the adjacent auxiliary pole to either side of the excitation stator pole, with a short flux path. In addition, when the phase current transitions from phase A to phase B, or from phase B to phase C or from phase C to phase A, there is no flux reversal in the stator of both structures and the core loss is uniform. Moreover, the asymmetrical property of radial stator poles of the 6/5 structure leads to unbalanced radial forces and causes larger vibrations, which Xu did not investigate in his work. On the other hand, the 12/8 segmental rotor SRM has two radially opposed stator poles symmetrically connected in series to form one phase with balanced radial electromagnetic forces. In fact, in static performance tests, the incremental inductance of the new segmented rotor SRM decreases gradually with increasing current, indicating that the new structure is more susceptible to magnetic saturation. The disadvantage of this design is that the slot area is too small. In [27,28], an 8-phase 24/18 segmental rotor SRM with 100 kW power for aircraft engines was designed. The rotor is embedded in a non-conductive hub ring made of high-strength material, and each segmental rotor can be divided into two rotor poles. The two adjacent

poles must be excited simultaneously, and when the motor's phases A and B are active simultaneously, a short closed magnetic path is formed between the stator pole and its aligned rotor pole, as shown in Figure 7c. Experimental results demonstrate that the core loss can be reduced by 40% compared to a CSRSM of the same capacity when the motor is operated at an ambient temperature of about 400 °C, with a power of 100 kW and a speed of 13,500 rpm. The reason for the reduction in core loss is that the flux flowing through the core is reduced during an excitation cycle, but the output torque of the motor also remains the same. However, due to its complex structure and higher manufacturing cost, as well as the high number of rotor poles and phases, this segmental rotor structure design may not be superior to the conventional structure; however, for machines operating in special environments such as gas turbines, the segmental rotor is a better choice.

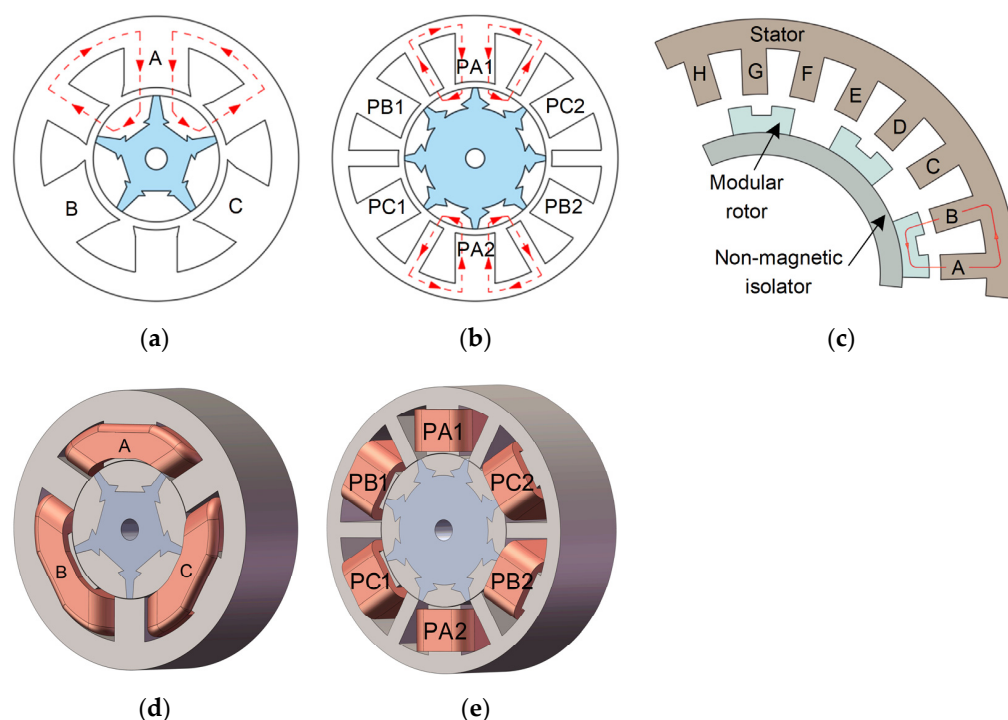


Figure 7. Proposed segmental rotor SRM with CW which used in vehicles cooling fans. (a) is the structure of the 6/5 segmental rotor SRM; (b) is the structure of the 12/8 segmental rotor; (c) is the 8-phase 24/18 SSRM with segmental rotors (1/3 model); (d,e) is the 3D model of segmental rotor SRM.

Sun proposed a four-phase 16/10 segmental rotor SRM for a belt-driven generator of vehicles as shown in Figure 8a [29], and conducted a systematic study of the structure. The connection of the stator windings was determined by the method of FEM [30], and the stator windings were connected by a concentrated winding with low mutual inductance between phases, which can increase the output of the motor. When a single-phase fault occurs, the new structure can generate 13% more torque than an SRM of the conventional structure and has low torque pulsation [31]. A new nonlinear aggregate parametric equivalent circuit model is proposed for the accurate calculation of iron losses [32], which investigates hysteresis, eddy current, and other stray losses using the energy conservation approach, and introduces incremental leakage inductance, incremental equivalent resistance, incremental magnetization inductance, and equivalent winding resistance to consider the effect of magnetic saturation on iron losses with high calculation accuracy. It can also be applied to other types of SRM. A 16/14 segmental rotor SRM was proposed [33] and compared with the 16/10 structure, as shown in Figure 8b. Experiments showed that the 16/14 structure has higher average torque and lower torque ripple at low speeds, and the 16/10 structure has slightly better performance at high speeds. A preliminary analysis of the selection of

the number of stator and rotor poles, as well as the size and number of winding turns of a segmented rotor SRM is presented according to the design method of a CSRSM [34,35]. Ref. [36] further investigated the electromagnetic modeling of a 16/10 segmented rotor SRM. It proposed a method to accurately calculate the 16/10 SSRM magnetic circuit based on the equivalent magnetic circuit approach, which includes the calculation of slot leakage reluctance, air gap reluctance, and core reluctance. The experimental platform was built using FPGA and compared with the finite element simulation results with high accuracy; the model can provide accurate real-time simulations for motor performance evaluation without motor prototype.

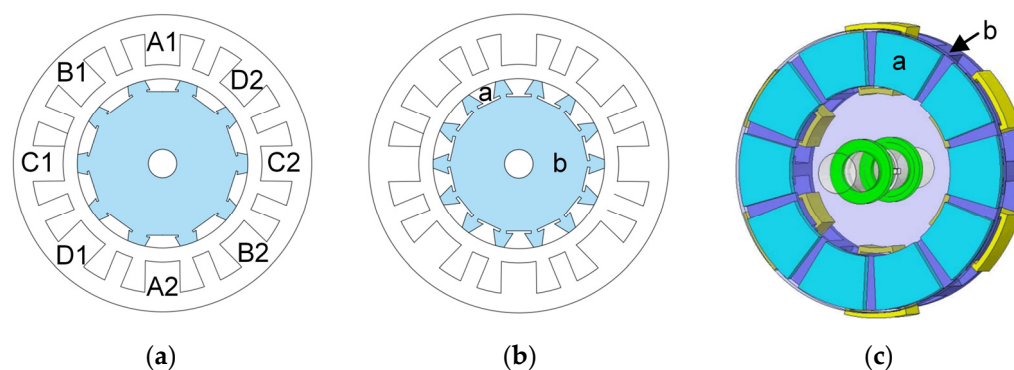


Figure 8. Proposed segmental rotor SRM with CW which used in a belt-driven generator of vehicles and 12/10 axial field SSRM. (a) is the structure of the 16/10 segmental rotor SRM; (b) is the structure of the 16/14 segmental rotor SRM where “a” depicts the segmented rotors and “b” is the non-magnetic isolator; (c) is the structure of the 12/10 segmental rotor AFSRM where “a” depicts the segmented rotors, “b” is stator core, and the yellow area is copper coils.

A three-phase 12/10 axial field switched reluctance motor (AFSRM) with a segmental rotor was designed as shown in Figure 8c [37,38]. Its stator poles are divided into excitation and auxiliary poles, with the magnetic flux closed through a shorter path. The design principle is similar to that of a radially structured segmental rotor SRM. Rotor segments are embedded in a non-magnetic isolator, reducing the weight and rotational inertia of the rotor. Due to its disk structure, the radial force can be neglected. However, the axial force during operation may cause the rotor to vibrate, making the air gap uneven and affecting the motor performance. A detailed analytical modelling of the structural magnetic circuit of a 12/10 axially segmental rotor SRM using the equivalent magnetic circuit approach [39] accurately calculates the air-gap permeability at the transition position between the aligned positions and the unaligned positions.

An external rotor SSRM was designed by Hall, and its basic structure is shown in Figure 9. An 18/15 external rotor segmented switched reluctance starter/generator was designed for an aero gas turbine [40]. The machine needs to operate at 350 °C and is capable of reaching an output power of 200 kW; the rotor segments are embedded in a fixed wedge-shaped tenon grommet for direct-drive in-wheel propulsion applications. In [41–43], a detailed study was conducted for externally segmented SSRMs which were designed to have a higher number of tooth poles and phases, such as 12/26 and 18/24 structures. Although the torque output capability and motor efficiency increased with the number of rotor segments, other performance parameters of the motor, such as the width of the weak magnetic zone and overload capability, decreased with the increase of rotor segments. This design overcomes the potential mechanical limitations with high-speed variants of this motor topology. It may be difficult to mechanically retain the rotor segments on an inner rotor due to high centripetal forces.

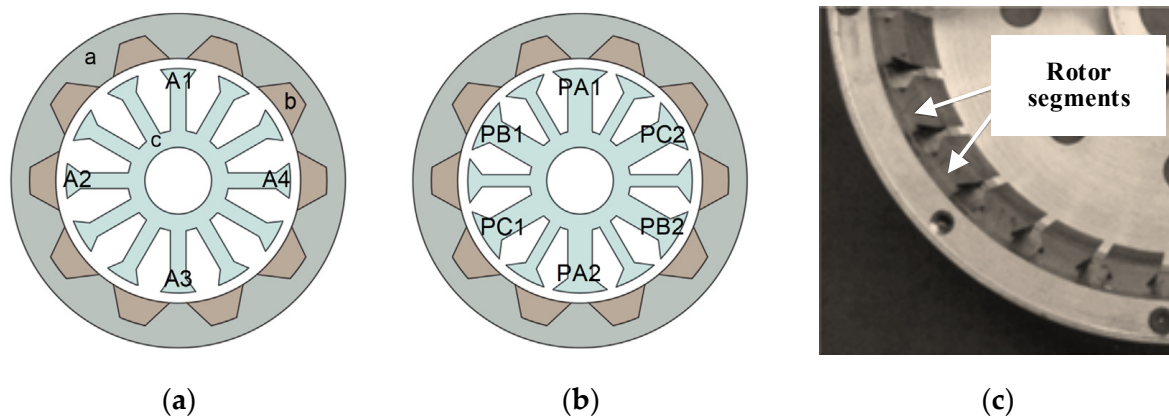


Figure 9. Schematic model of external segmented rotor SRM. (a) is FPW connection where “a” is the rotor sleeve and “b” the is outer segmental rotor, “c” is inter segmental rotor; (b) is the CW connection; (c) is the prototype of the rotor.

2.1.2. Control of Segmental Rotor Type

There is little research on control methods for segmented structures. Zhang has studied the control system of the 12/8 segmented rotor SRM [44], and the control scheme is shown in Figure 10. The whole system adopts closed-loop speed control and controls the switching on or off of each phase according to the rotor position information fed back in real time by the encoder fixed on the rotating shaft. The speed is fed back to the PI module in real-time for comparison with the given speed. When the measured speed is higher than the given speed, the PI module will decrease the duty ratio of PWM to reduce the motor speed. If it is lower than the pre-given speed, the PI module will increase the duty ratio of PWM to increase the motor speed. Depending on the rotor position signal that is fed by the encoder, the phases of the motor will be excited alternately. The motor current measured by the current sensor will be fed to the PWM generator module, when the load current is greater than the limited current, the PWM signals will be turned off to protect the drive system.

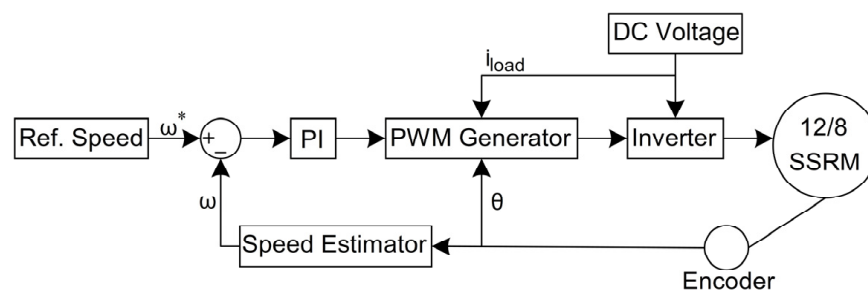


Figure 10. The control scheme for the 12/8 SRM with CW and segmental rotor. Notes: ω^* is rotor’s reference angular velocity; ω denotes angular velocity; θ represents rotor position; i_{load} means the motor current with load.

Chen made a preliminary design of the digital control system for such a structure [45], including a power converter, position detection, protection circuit, etc. The control block diagram of the system is shown in Figure 11. The traditional method of closed-loop control of speed is adopted, including current chopper control at a low speed and angular position control at a high speed. The angle calculation module is used to calculate the rotor position and judge the phase switching signal. Combined with the current chopper signal from the current chopper module, the logic judgment module can generate the drive signal. Torque calculation is a finding module. Known current and rotor position can be found according to the motor’s torque angle curve to find the corresponding torque magnitude.

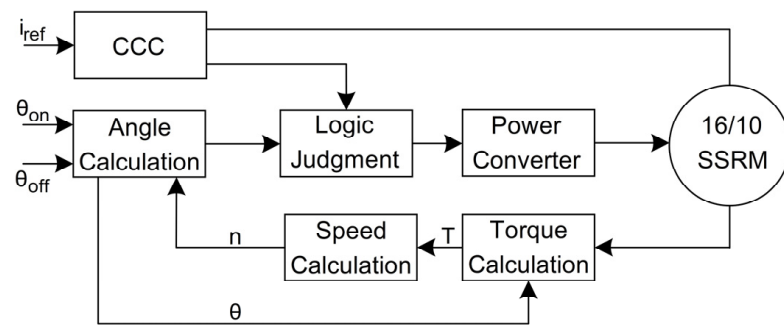


Figure 11. The basic control diagram of the digital control system of 16/10 SSRM. Notes: θ_{on} , θ_{off} , and θ denote turn-on, turn-off angle, and rotor position, respectively.

The torque of SRM is usually controlled indirectly by traditional control methods, such as current chopper control at low speed and angular position control at high speed, by controlling the phase current or adjusting the turn-on or turn-off angle to control the torque and suppress the torque ripple. However, it is possible to use some advanced control strategies to improve the motor's dynamic performance. Direct torque control (DTC) is proposed to suppress the 16/10 segmental rotor SRM's torque ripple [46] with the control block diagram shown in Figure 12. Moreover, a double closed-loop structure is used, where the given speed ω^* and the actual speed ω form the speed loop, and the reference torque T^* and the actual output torque T are the outputs of the controller to form the torque loop for the purpose of controlling the torque. The difference between the given value and the actual value is limited to the hysteresis loop width. As such, the sector where the current synthetic magnetic flux-linkage vector is located is calculated, and the increase or decrease of torque and magnetic flux-linkage is also determined. Then the appropriate spatial voltage vector is selected by querying the switch table to control the switch off of each phase of the motor, thus achieving control of torque and magnetic flux-linkage and suppressing motor torque pulsation. Compared with the traditional current chopping strategy, the speed waveform fluctuation of the DTC strategy is smaller after reaching the rated speed, and the speed drops less when the load changes abruptly and the response time is shorter. This means the robustness of the DTC strategy outperforms the traditional current chopping control strategy.

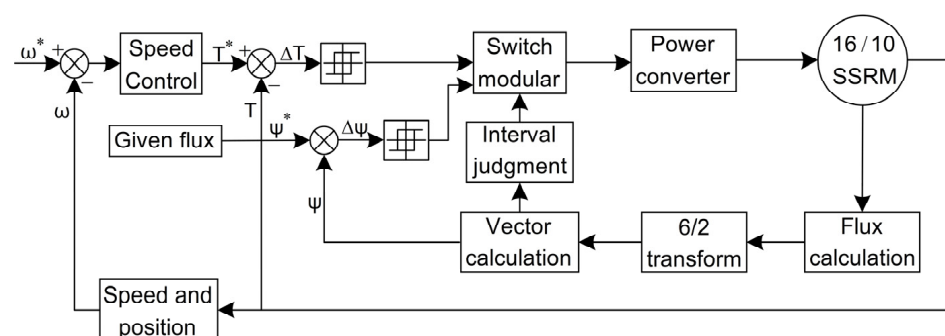


Figure 12. Control block diagram of the DTC system of 16/10 SSRM. Notes: ψ is given flux; ψ^* is the actual flux.

Direct instantaneous torque control (DITC) reduces torque pulsation by the transient response of the torque lag controller. An improved direct transient torque control method is proposed in [47], which uses adaptive terminal sliding-mode control (ATSMC) based on the rate of load change in order to improve the direct transient torque control system, and the control block diagram of the system is shown in Figure 13. The sliding-mode control is more sensitive to internal parameter changes and external disturbances. It mainly includes the reasonable selection of the sliding-mode surface and the design of the control input,

such the state point of the system is gradually stabilized to the equilibrium point along the phase trajectory. The traditional exponential convergence law can be expressed as:

$$\dot{s} = -\varepsilon \operatorname{sgn}(s) - ks, \quad \varepsilon > 0, k > 0 \tag{2}$$

where, $\varepsilon \operatorname{sgn}(s)$ denotes the isokinetic approximation term, ks represents the exponential approximation term, and ε and k represent switching gain and linear gain, respectively. The increase in k in the remaining states accelerates the arrival speed and sliding jitter, except for the case when the system state is close to the sliding membrane switching surface when ks is almost zero. In order to avoid the contradiction between the two, a new convergence law is proposed as in (3), where x indicates system status and α and β are variable term factors. In the novel convergence law, the variable term gains as the system approaches the sliding mode surface, $|x|/(|x| + \alpha)$ gradually decreases and eventually converges to 0, but $\varepsilon|x|/(|x| + \alpha)$ always smaller than 1. Jitter is reduced and control performance is improved. A second-order terminal sliding mode controller based on a novel convergence law is designed to speed up the response time and improve the immunity of the system to disturbances when the internal parameters change. Adaptive estimation of the load torque rate of change allows real-time estimation of disturbances, maintains system robustness, and reduces the switching gain to reduce torque pulsation.

$$\dot{s} = -\frac{\varepsilon|x|}{|x| + \alpha} \cdot |s|^\beta \operatorname{sigmoid}(s) - k|x| \cdot s \tag{3}$$

$$\lim_{x \rightarrow \infty} |x| = 0, \quad \varepsilon > 0, k > 0, \alpha > 0, 0 < \beta < 1 \tag{4}$$

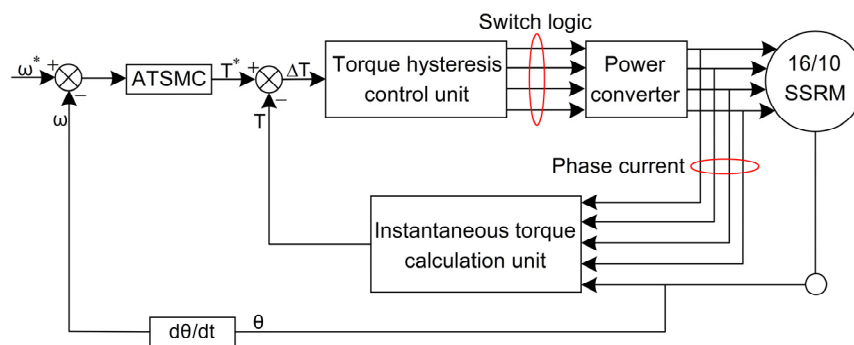


Figure 13. Control block diagram of the improved DITC system based on ATSMC that is used in 16/10 SSRM.

2.1.3. Electromagnetic Design of Segmental Rotor Type

The main dimensions of the motor include the rotor outer diameter D_r and the stack length h . The relationship between the rotor outer diameter and the stack length can be expressed as (5):

$$\lambda = \frac{h}{D_r} \tag{5}$$

where λ is the slenderness ratio. Normally, it usually takes values between 0.5~3. In addition, D_r and h can also be expressed as (6) [33]:

$$D_r^2 \cdot h = k \cdot \frac{6.1P_{em}}{B_\delta A} \tag{6}$$

where k is experience factor, B_δ is magnetic loading, A is electric loading, and P_{em} is electromagnetic power. Then, the main dimensions of the segmental rotor SRM can be initially determined. The stator poles of the segmental rotor SRM with single tooth structure are divided into excitation poles and auxiliary poles in order that, in the electromagnetic design, certain constraints should be satisfied between the basic parameters of the stator

and rotor segments. Moreover, the basic parameters should meet the relationship described below under the premise of ignoring the inter-phase leakage, with the basic structure diagram shown in Figure 14a.

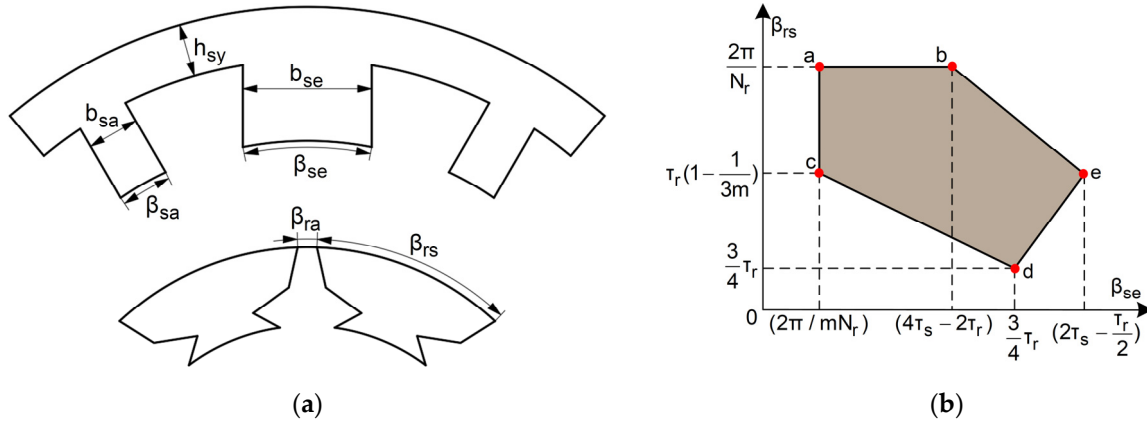


Figure 14. (a) Basic structure diagram of segmental rotors SRM with ST windings; (b) Reasonable constraint quadrilateral of SRM with segmental rotors. Notes: point a $(\frac{2\pi}{mN_r}, \frac{2\pi}{N_r})$; point b $(4\tau_s - 2\tau_r, \frac{2\pi}{N_r})$; point c $(\frac{2\pi}{mN_r}, \tau_r(1 - \frac{1}{3m}))$; point d $(\frac{3}{4}\tau_r, \frac{3\tau_r}{4})$; point e $(2\tau_s - \frac{\tau_r}{2}, \frac{2\tau_s - \tau_r}{2})$.

- The numbers of stator poles and rotor segments should follow (7), where LCM is the least common multiple of the number of stator poles N_s and the number of rotor poles N_r . If the number of rotor segments is too small, the leakage flux is serious, and the motor will have poor startup ability due to the large angle between the two adjacent segmented rotors. If the number of rotor segments is larger, the rotor pole is too small to meet the requirements.

$$\text{LCM}(\frac{1}{2}N_s, N_r) = mN_r \tag{7}$$

- At the aligned position, the excitation pole arc β_{se} is equal to the sum of twice the auxiliary pole arc β_{sa} and the rotor segment inter-pole arc β_{ra} , and the rotor segment pole arc β_{rs} is less than one rotor pole pitch, which can be expressed as (8).

$$\beta_{se} \geq 2\beta_{sa} + \beta_{ra} \tag{8}$$

- In order to prevent mutual coupling between phases, the flux of one phase flows into the excitation pole of the adjacent phase during excitation. To maximize the flux generated by the excitation winding to the adjacent auxiliary pole, the stator and rotor pole arcs at the aligned position should satisfy (9), where $\tau_s = 2\pi/N_s$ is the stator pole pitch.

$$\tau_s + \frac{1}{2}(\beta_{sa} - \beta_{ra}) < \beta_{rs} < 2\tau_s - \frac{1}{2}(\beta_{se} + \beta_{ra}) \tag{9}$$

- The auxiliary pole arc β_{sa} should be larger than the arc between rotor segments arc β_{ra} to prevent the core electromagnetic utilization rate from being too low.

$$\beta_{sa} \geq \beta_{ra} \tag{10}$$

- Meanwhile, to ensure that the motor can be in any position with forward or reverse self-starting ability, it usually requires that the rotor segment pole arc β_{rs} be greater than the excitation pole arc β_{se} and not lower than the motor step angle, with the step angle expressed as $2\pi/(mN_r)$.

$$\beta_{rs} > \beta_{se} > \frac{2\pi}{mN_r} \quad (11)$$

Combined with the above constraints, a reasonable constraint polygon between the rotor segments pole arc and the excitation pole arc or auxiliary pole arc can be drawn as shown in Figure 14b.

The SSRM's windings are only wound on the excitation pole; the auxiliary pole is only used as the return path of the magnetic flux, so the width of the excitation pole b_{se} should be equal to twice the width of the auxiliary pole b_{sa} . The stator yoke thickness h_{sy} and the rotor segment height h_{rs} should be greater than or equal to the auxiliary pole width b_{sa} to prevent oversaturation of the yoke, which can be expressed as:

$$b_{se} \geq 2b_{sa} \quad (12)$$

$$h_{sy} \geq b_{sa} \quad (13)$$

$$h_{rs} \geq b_{sa}. \quad (14)$$

The number of series turns per phase winding is expressed as (15).

$$N_{ph} = \frac{N_r U \cdot 0.5(\tau_r - \beta_{rs})}{\omega B_\delta D_r h \pi} \quad (15)$$

The slot fill factors of the SSRM with segmented rotors can be calculated as (16):

$$S_f = \frac{\pi d_{coil}^2 N_{ph}^2}{8 \cdot \left\{ \pi \left[\left(\frac{D_{s1}}{2} - h_{sy} \right)^2 - \frac{D_{s2}^2}{4} \right] - 3D_{s2} \left(\frac{D_{s1}}{2} - h_{sy} - \frac{D_{s2}}{2} \right) (\beta_{se} + \beta_{sa}) \right\}} \quad (16)$$

where d_{coil} is the diameter of the copper wire, D_{s1} is stator inner diameter, D_{s2} is stator outer diameter, and h_{sy} is stator yoke height. Due to the highly nonlinear nature of segmental rotor SRM, the electromagnetic torque can be expressed as (17), where a model is analyzed first using a linear inductance model and neglecting edge effects and magnetic saturation. In (17), W_m is magnetic co-energy, L , i , and θ indicate inductance, phase current, and rotor position angle, respectively.

$$T = \frac{\partial W_m}{\partial \theta} = \frac{1}{2} \frac{\partial L}{\partial \theta} i^2 \quad (17)$$

We can use inductance at aligned and unaligned positions, L_{max} and L_{min} , to approximate the magnitude of the average torque. $\tau_r = 2\pi/N_r$ is the rotor pole pitch.

$$T_{av} \approx \frac{1}{\tau_r} i^2 (L_{max} - L_{min}) = \frac{i^2}{\tau_r} \Delta L \quad (18)$$

$$T \propto N_r \cdot (L_{max} - L_{min}) \quad (19)$$

The simplified torque expression is proportional to the phase current i and variation of inductance ΔL , which can be used for initially estimating the torque of the designed SSRM.

2.2. Segmental Stator Type

By replacing the conventional continuous core structure of SRM with a segmented structure, the SSRM has a shorter magnetic flux diameter. Therefore, the new structure can reduce the MMF requirement and core loss without increasing the number of phases or poles. In addition, due to the segmented structure, some flux paths in adjacent positions of the motor can be magnetically isolated, thus improving the reliability and fault tolerance of the motor. Therefore, the segmented form of SRM is superior to the conventional structure. In addition to the segmental rotor structure, the segmental stator structure has also been investigated. Similar to the rotor segmentation, the stator core is divided into two or N discrete stator segments.

Also, a new two-phase 6/10 segmental stator SRM is proposed in [48]. The stator is divided into two separate stator segments, as shown in Figure 15a. The windings are wound on both ends of the E-type stator teeth. The common pole of the E-type stator serves as a path for the flux return from both ends, forming the same short flux path as the segmented rotor SRM, and without flux reversal in the stator during phase winding commutation, thereby reducing core loss. The special feature of this structure is that the reluctance under the common pole is always kept minimum no matter the position to which the rotor is turned. This is because the area swept by the convex pole of the rotor over the surface of the common pole is kept constant, which can be regarded as the common stator pole and the rotor pole always being in a completely overlapping position. The total reluctance of the magnetic circuit is inversely proportional to the electromagnetic torque, so this structure can achieve higher torque with balanced radial force. No other special bearing support is needed. As such, the amount of stator iron is reduced by 22%. The power density is also higher, which is suitable for some low-cost and high-capacity drive applications. However, ten rotor poles increase the switching frequency of the motor drive circuit, which will limit the performance of the motor at high-speed operation.

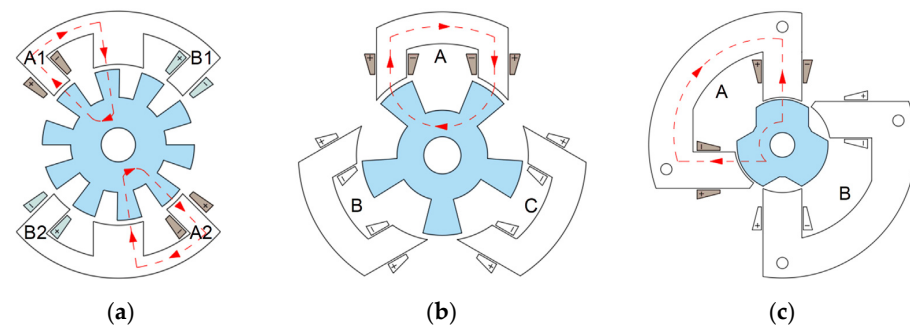


Figure 15. SRM with segmental stators. (a) is 6/10 with E-core stators; (b,c) are 6/5 and 4/3 C-core stators which are used in high-speed applications, respectively.

For this purpose, 6/5 and 4/3 structure C-type segmental stator SRM [49,50] are proposed for high-speed drives, as shown in Figure 15b,c. The 6/5 C-type segmental stator structure reduces the number of rotor poles by half compared to the 6/10 E-type structure. The switching frequency is reduced; however, during excitation, the flux flows only on one side of the motor, which leads to unbalanced magnetic pull on one side and high vibration noise. At the same time, in order to ensure that the magnetic flux can flow into the rotor as much as possible, the rotor pole arc in the alignment position should be greater than or equal to the arc of the C-type stator pole. Therefore, it is suitable for some applications that require high torque but not high vibration and noise requirements. The 4/3 segmental stator structure uses an inhomogeneous air gap, which increases the positive torque region of the motor without torque dead zone, and the 4/3 segmented structure has a higher magnetomotive force compared to the conventional 4/2 structure SRM under the same size and flux density limitation, resulting in a higher output torque [51]. The high torque, high efficiency, and asymmetry of the positive and negative torque regions make it suitable for unidirectional high-speed rotation, such as blower applications. Lobo extends the segmental stator SRM to the M-phase N-segments [52], with flux-reversal-free-stator (FRFS), as shown in Figure 16. By changing the flux direction of adjacent stator poles, no flux reversal of the stator core is achieved, and each stator segment carries an equal amount of flux during excitation with a balance radial force. The distance between two stator segments should be larger than the distance of the air gap between the stator and rotor to minimize the magnetic leakage between stator segments.

Figure 17a shows a SRM with the stator segments in the axial direction, where eight C-type segmental stators are uniformly arranged around a double-layer rotor section [53] and two diametrically opposite stator segments are connected in series to form one phase with the magnetic flux passing through the axial stator yoke on both sides, and the upper

and lower rotor and the air gap on both sides are connected to form a circuit, as shown in Figure 18a. The path is relatively long, which is not conducive to reducing the core loss. The C-type stator segment omits the radial stator yoke section, which uses less core material, and the magnetic circuits are independent between each phase and each stator segments, which has electrical isolation capability and increases the reliability of the motor. The wire is wound on the yoke part of the C-type stator segment, which is straightforward and convenient to wind. However, because it is exposed on the outside of the stator, it is actually equivalent to increasing the outer diameter of the motor. The length of the magnetic circuit in the axial direction is considerable and the axial utilization is low, which is not suitable for applications with sizeable axial length. Compared to an SRM with the same slot fill factors, the stator slot winding area is larger, allowing more wires to be wound and a higher output torque capability at the same current. It can also be considered that less current is required to output the same level of electromagnetic torque compared to CSRSM. Even though there are more turns of wire per phase, the copper loss is still at a lower level because copper loss is proportional to the square of the current. The current level is lower, so the copper loss is also lower than conventional structures.

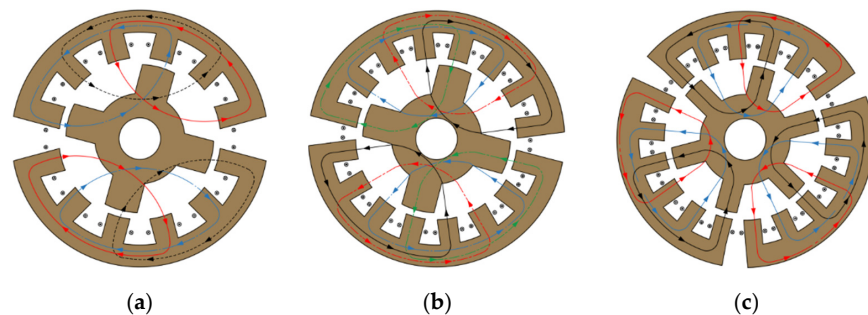


Figure 16. Structures of FRFS-SRMs. (a) three phase two segments SRM; (b) four phase two segments SRM; (c) three phase and three segments SRM.

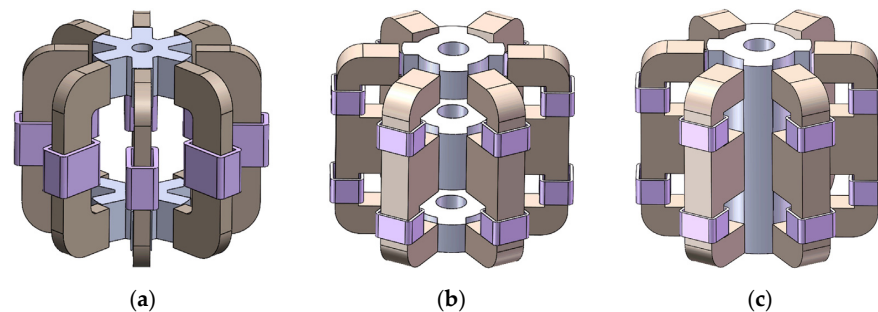


Figure 17. The model of SRM with segmental stators. (a) is 8/6 with C-shape segmental stators; (b) is 6/4 with E-shape segmental stators and triple axial segmental rotor; (c) is 6/4 with E-shape segmental stators which used solid axial rotor.

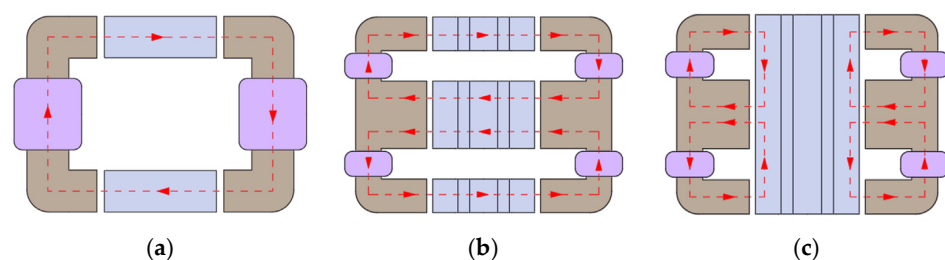


Figure 18. The flux paths of SRM with segmental stators. (a) Flux paths in 8/6 C-shape segmental stator SRM; (b) Flux paths in 6/4 E-shape segmental stator SRM with triple axial segmental rotor. (c) Flux paths in 6/4 E-shape segmental stator SRM with solid axial rotor.

To address the problem of low axial utilization of the C-type stator segment, Ding proposed an E-type segmental stator SRM with two different structures, a three-layer segmental rotor [54] and a solid rotor [55], as shown in Figure 17b,c. Six individual E-type segmental stators are uniformly wrapped around the rotor. The windings are wound in two grooves of the E-type stator teeth with two diametrically opposite segmental stators connected in series as one phase. In Figure 18b, it can be seen that the three-layer segmental rotor structure has two flux paths: one from the upper rotor, upper E-type stator pole, upper air gap, and stator yoke to the middle rotor return; the other one from the lower rotor, lower E-type stator pole, lower air gap, and stator yoke to the middle rotor return, which is equivalent to passing the motor outer diameter in the radial direction with a longer path. There is an axial magnetic path in the rotor, and both radial and axial magnetic paths in the stator. On the other hand, the solid rotor structure has four paths, as shown in Figure 18c, with the upper and lower paths symmetrically distributed. All flux paths of both rotor structures return at the middle pole of the E-type stator, so the height of the middle tooth pole is at least the sum of the height of the top and bottom poles, and the width of the stator yoke should also be equal to the width of the top and bottom poles to prevent oversaturation of the stator yoke. The magnetic paths of segmental stator SRM are relatively simple, and the equivalent magnetic path method can be used to model the equivalent magnetic paths of both rotor structures at aligned and unaligned positions to accurately calculate the magnetic flux-linkage [56,57]. There is no radial stator yoke in the E-type stator module. The amount of iron in the stator is 24.9% lower compared to the CSRSM, which further reduces the overall weight of the motor and increases the torque density. In terms of static performance, the segmental stator SRM with both rotor configurations has higher torque output capability than the CSRSM and can input higher MMF, but the higher MMF causes the motor to saturate more easily under high excitation currents.

The segmental stator SRMs with both rotor configurations are almost identical in terms of dynamic performance. Both produce higher average torque, with the triple segmented rotor structure having higher torque density due to its 18.7% lower weight than the solid rotor structure and high self-starting capability. The windings of both E-type stator and C-type stators are wound radially in the groove of the stator segment, which is convenient to wind and easy to automate. However, this characteristic leads to an increase in the radial length of the motor. A segmental stator SRM in the form of a single winding is proposed in the literature [58]. The rotor is still divided into a three-layer segmental rotor. The magnetic flux path is similar to that of the segmental stator SRM with double-winding configuration. The coil is wound on the middle pole of the E-type stator, so the segmental stator SRM with the single-winding configuration is smaller in size than the segmental stator SRM with the double-winding configuration. This can be suitable for applications with high space constraints, but winding can be complicated and is not conducive to industrial automation production. The three stator poles at the top, middle, and bottom of the E-type segmental stator generate force on the rotor and drag the motor to rotate, which has the following advantages: large stator winding space allowing winding more coils, which improves the input MMF of the motor; magnetic and thermal isolation between each phase, with strong electrical isolation and good fault tolerance performance; no coupling between adjacent phases, omitting the radial stator of the traditional motor yoke part, which reduces the weight of the motor. Based on these advantages, especially safety and high fault tolerance, the segmental stator SRM can be used in some applications with high safety requirements [59,60] and can also be deployed in some industrial applications with high torque and high power density requirements, such as electric/hybrid vehicles. In addition, as seen in Figure 18c, when the segmental stator SRM winding is excited, the flux path in the solid rotor structure does not pass through the rotor yoke; it only flows in the rotor teeth, so the solid rotor can be designed in the form of the axially divided segment, as shown in Figure 19. The rotor segments are embedded in a non-magnetic isolator, which uses less core material, thereby reducing the wind resistance at high speed of the motor. However, the manufacturing difficulty of the motor is increased.

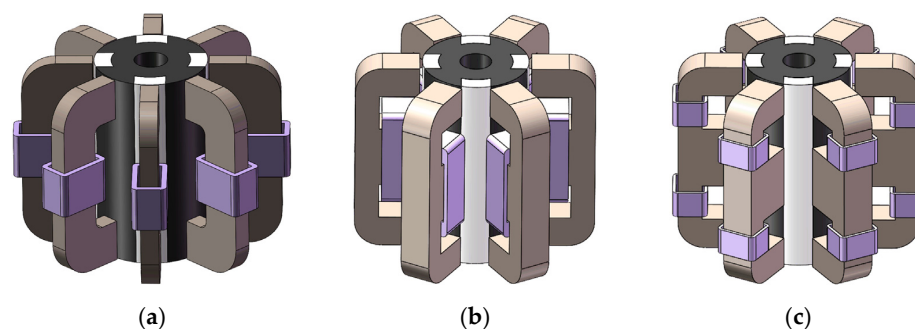


Figure 19. Segmental stator SRMs with radial segmental rotors. (a) 8/4 segmental stator SRM; (b,c) are 6/4 segmental stator SRMs with single coils and double coils, respectively. Notes: the white area represents the segmental rotors, whereas the black area is the non-magnetic isolator.

3. New Type of Segmental SRM

3.1. Double-Stator SSRM

The SRM relies on the change in the air gap reluctance between the stator and rotor to generate torque. The electromagnetic force in the air gap is divided into two types, one is the tangential electromagnetic force used to generate torque, and the other one is the radial electromagnetic force that triggers vibration noise. In order to optimize the electromagnetic force in the air gap to produce the tangential electromagnetic force and weaken the radial electromagnetic force as much as possible, some researchers proposed the double-stator segmental switched reluctance motors (DSSRM) [61–64] based on the optimization of the electromagnetic force in the air gap, which has a stator structure consisting of an outer stator and an inner stator, a rotor comprising of multiple discrete rotor segments, and stator windings that can be connected with FPW or CW [65]. The magnitudes of radial and tangential electromagnetic forces in the air gap were calculated by the maxwell stress tensor method, showing that the double-stator structure increases the tangential electromagnetic force of the motor and weakens the radial force, thus increasing the electromagnetic torque.

A new double-stator segmented SRM [66] has been proposed based on the conventional double-stator SSRM, combining the advantages of the segmented structure, as shown in Figure 20a. The outer stator consists of six U-shaped segmental stators, where each outer stator module contains two stator poles, and the 12 teeth of the inner stator still adopt the traditional convex pole structure. Both the inner and outer stators are connected with CW, and the outer stator winding is wound at both ends of the U-shaped stator. The diametrically opposite poles are connected in series as one phase, and the magnetic flux passes through one pole of the U-shaped stator. It flows in the segmental rotor and air gap, after which it passes through the inner stator and returns to the other pole of the U-shaped stator. The double-stator SSRM reduces the amount of iron compared to the conventional double-stator SSRM, and the modules are isolated from each other without coupling. This shortens the flux path, reduces core losses, and improves the fault tolerance of the motor. It combines the advantages of segmented stator and double-stator structures, outperforms the conventional double-stator SSRM in terms of average torque and torque pulsation, and is suitable for applications that require high torque and low ripple, such as electric vehicles. However, the magnetic flux generated by the inner and outer stator will be coupled at the rotor segments, resulting in a high magnetic flux density of the rotor segments. Cheng has improved the stator structure of the double-stator SSRM with a U-shaped segmented structure for both the inner and outer stator [67–69], as shown in Figure 20b. This structure can be viewed as a combination of an outer rotor segmented stator SRM and an inner rotor segmented stator SRM with three excitation modes, inner stator alone, outer stator alone, and inner and outer stator simultaneously. When the outer (inner) stator is separately excited, the magnetic flux passes through the two poles of the outer (inner) stator, the rotor cam, rotor yoke, and air gap, with no coupling between the inner (outer) stator. The electromagnetic torque when the inner and outer stator are excited

simultaneously is equal to the sum of the electromagnetic torque when they are excited separately. Moreover, the aligned and unaligned positions of the inner and outer stators occur at the same moment. So, the total maximum (minimum) electromagnetic torque is equal to the sum of the maximum (minimum) torque when the inner and outer stators are separately excited, which leads to a large torque pulsation in this structure. When two diametrically opposite inner and outer stators are excited simultaneously, the magnetic flux-linkage generated by the inner and outer stators are coupled to each other and part of the magnetic flux flows in the yokes of the two adjacent rotors. Therefore, in order to avoid excessive torque pulsation and the problem of rotor yoke oversaturation due to mutual coupling of the inner and outer stator, the inner and outer convex poles of the rotor can be staggered by a certain mechanical offset angle θ , and the conduction sequence of the inner and outer stator windings can be reasonably arranged, as shown in Figure 20c. When the outer stator reaches the maximum (minimum) torque position, the inner stator is at the minimum (maximum) torque position, which can effectively reduce the torque ripple, but will lower the average torque of the motor. Reasonable arrangement of the phase of the inner and outer stator can realize the decoupling of the inner and outer stator fields in one rotor cycle, which is easy to control.

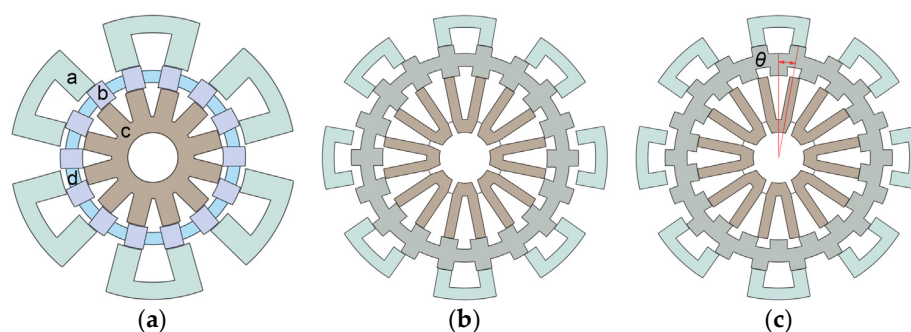


Figure 20. (a) 12/14/12 double-stator SRM with segmental outer stators and rotors where “a” and “b” are U-shaped segmental stators and segmental rotors, respectively, “c” is inner stator and “d” is non-magnetic isolator; (b,c) are proposed 16/18/16 double-stator SSRMs with inner and outer segmental stators without non-offset and with offset rotors.

To further optimize the performance of DSSRM, FEM analysis was used to evaluate the effect of rotor segment pole arc size on motor performance [70]. For rotor segment shape, internal rotor slotting, asymmetric rotor shape, and rotor layering were proposed [71–73] which effectively reduced torque pulsation and increased the average torque. Both the previously mentioned segmental stator or rotor structure and dual-stator SSRM can effectively improve the performance of the motor.

3.2. Bearingless SSRM

As is well known, BSRM has both torque and levitation force windings wrapped around the stator teeth. The torque and levitation force are coupled when the windings are excited, which increases the control difficulty. Peng proposed a double-stator BSRM [74], in which the inner stator generates the levitation force and the outer stator generates the rotating torque. Compared with the conventional BSRM, this structure further separates the torque flux and the levitation force flux spatially, especially the mixing of the two fluxes rarely occurs in the stator. As such, the degree of decoupling is greatly improved and the control difficulty is reduced. At the same time, radial force pole arc of this structure is much larger than the previous structure, so it can produce stable radial force at any rotor position, and the control method of the levitation force is simplified.

On this basis, Huang proposed a double-stator segmental rotor BSRM [75], as shown in Figure 21a, where the rotor consists of a fan-shaped rotor segment, a spacer sleeve, and an annular core, which not only weakens the coupling between the torque and the levitation system, but also improves the torque output capability compared with the conventional

double-stator BSRM. However, due to the use of the FPW, the winding ends overlap each other, making the ends larger and increasing the end effect of the motor. To address this problem, Xu proposed a new double-stator segmental rotor BSRM with CW [76,77] which combines the advantages of a short flux path and no flux reversal in a segmental rotor SRM, as shown in Figure 21b. The structure has two stators, with the outer stator core divided into excitation and auxiliary poles for generating electromagnetic torque, the inner stator used to generate the levitation force, and the rotor segment embedded in the isolator. Because of the special structure, compared with the long magnetic circuit structure of the conventional double-stator BSRM, the new structure operates under a short flux path and does not have flux reverse in the outer stator when the torque windings change phases, thus improving the torque density, reducing the MMF requirement of the motor and decreasing the iron loss, thereby contributing to improving the efficiency of the motor. At the same time, the torque flux and levitation force flux of the motor is further separated in space by the rotor spacer sleeve. The coupling degree of the magnetic path is further weakened, which is conducive to the decoupling control of torque and levitation force, reducing the control difficulty of the motor.

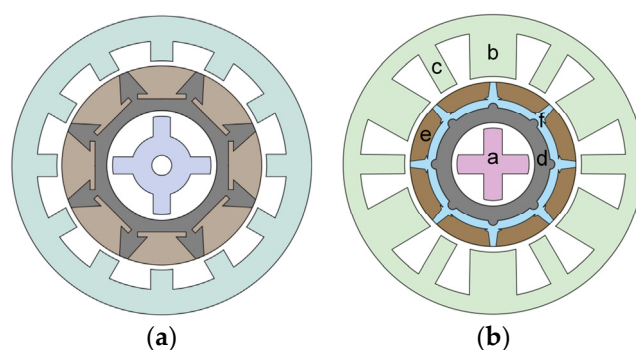


Figure 21. (a) is a 12/8 BSRM with segmental rotors and FP winding; (b) is a 12/8 BSRM with segmental rotors and ST winding where “a” is inner stator, “b” and “c” are the excited pole and auxiliary pole of the outer stator, respectively, “d” is toroidal iron core, “e” is the rotor segment, and “f” is the non-magnetic isolator.

3.3. Hybrid Excitation SSRM

Both the segmented structure and the double-stator structure can effectively reduce the torque ripple of the motor and improve the average torque, but they are still inferior to the permanent magnet motor in terms of power density and efficiency. Some researchers have proposed that the performance of the motor can be improved by embedding permanent magnets between the stator teeth, stator yoke, or stator tooth poles [78–81]. The SRM usually works in the first quadrant of the B-H curve of the iron core material. After adding permanent magnets, the motor can work in the first and third quadrants of the iron core material, and the maximum saturation magnetic density increases, which reduces the magnetic saturation of the stator iron core. An 8/10 two-phase permanent magnet-assisted SRM is proposed in [82], where the stator core is divided into a torque pole and a common pole, and the stator winding is connected by CW. Permanent magnets embedded in the stator yoke on both sides of the common pole, and the winding is wound on the torque pole only, with the common pole providing the path for flux return. A prototype was designed and manufactured for experiments, and it was demonstrated that the new structure could effectively increase the average torque with no flux reversal. In the literature [83], a 6/10 hybrid excitation SRM was proposed with one permanent magnet placed in each stator slot, which reduces magnetic saturation and increases the flux density in the air gap, thus increasing the electromagnetic torque.

To further enhance the power density of the hybrid excitation SRM, a three-phase 12/8 hybrid excitation segmented switched reluctance motor (HESSRM) has been proposed by combining the segmented stator structure and permanent magnets, as shown in

Figure 22a. Each U-shaped stator segment is equipped with rare earth permanent magnets between the two poles, and four diametrically opposite coils are connected in series as one phase, meanwhile the rotor is a conventional convex pole structure. The flux paths of the 12/8 HESSRM without phase winding excited and with phase winding excited are shown in Figure 22b,c, with the red arrows indicating the direction of magnetization of the permanent magnets, the blue arrows indicating the direction of flux generated by the windings, “-” indicating the current flowing into the paper, and “+” indicating the current flowing out of the paper. As Figure 22b,c shows, when the winding is not energized, the flux generated by the permanent magnet is closed through the yoke of the stator segment. When the winding current is energized, the flux generated by the permanent magnet is superimposed with the flux generated by the winding at the air gap, increasing the electromagnetic force and outputting higher electromagnetic torque even at lower current levels [84–86]. Despite the addition of permanent magnets between the stator poles, the weight is still 9.4% lower than that of the CSRSM. The torque output capability is high and the power density further increased. Furthermore, it can be seen from Figure 22b that when the coil is unexcited, there is almost no magnetic flux through the air gap and rotor, so the cogging torque of this structure is small and does not contribute to torque pulsation and vibration noise. The outer stator has more space to wind more windings and leaves some space to design the cooling system of the motor. In addition to the U-shaped stator, there is also the A-shaped stator core structure [87] which has achieved similar results. In [88], Kondelaji proposed a permanent magnet assisted double-stator SSRM as shown in Figure 23. The basic structure and the connections of the windings are the same as those of the conventional double-stator SSRM. Still, the torque is improved due to the presence of permanent magnets; however, the torque ripple is not well suppressed, and the cost of the motor is increased, rendering it unsuitable for industrial applications.

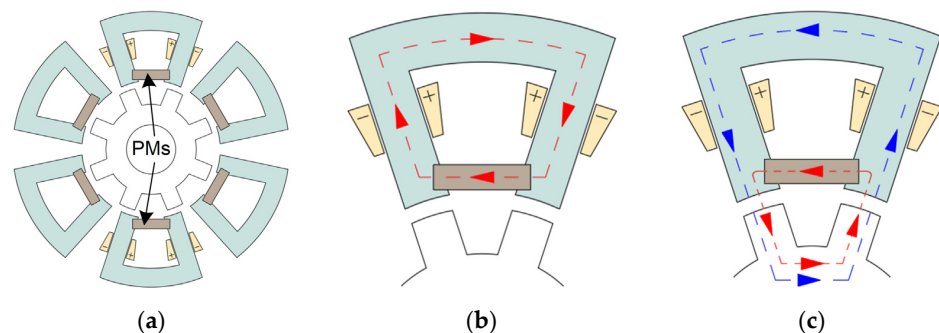


Figure 22. Proposed new type of 12/8 HESSRM. (a) is the basic structure; (b,c) are the flux paths without phase winding excited and with phase winding excited, respectively.

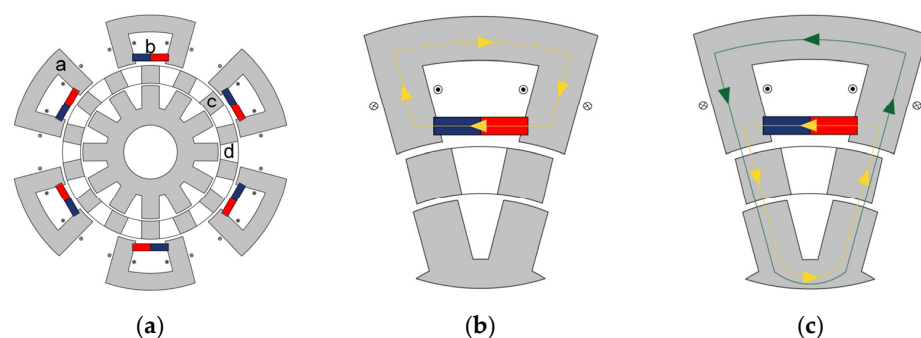


Figure 23. PM assisted DSSRM with segmental outer stator and rotor (a) is a simplified model where “a” is the U-shaped segmental stator, “b” depicts PMs, “c” is the segmental rotor, and “d” is the non-magnetic isolator; (b,c) are the flux paths without phase winding excited and with phase winding excited, respectively.

Table 1 gives the advantages, disadvantages, and applications of all types of SSRM presented above. Moreover, linear switched reluctance motors (LSRM) are also an important branch of SRMs with structural variants similar to rotation SSRMs. The stator structure can still be divided into two structures according to windings' connections, i.e., equal-tooth and unequal-tooth forms. What is more, there are double mover structures with FPW and CW [89,90], and double mover segmented LSRM with toroidal windings [91], but the analysis of segmented LSRM is not summarized in this paper and will be researched in future work.

Table 1. Comparison of advantages, disadvantages, and applications of various SSRMs.

SSRM Topologies	Winding Topologies	Advantages	Disadvantages	Applications
(Radial field) segmental rotor type	FPW [10,13,18]	<ul style="list-style-type: none"> High output torque compared with CSR Short flux path Low MMF requirement High electromagnetic utilization No mechanical protrusion on the rotor surface 	<ul style="list-style-type: none"> Longer end winding resulting in low utilization rate of the winding, low electric loading, and low reliability of the motor Poor heat dissipation performance at end winding Flux reversal in stator pole Complex rotor assembly 	<ul style="list-style-type: none"> Aerospace, automotive, military, and household applications Not suitable for applications with short lamination stack length and large pole pitches
	CW [22,24,26,33,35,44]	<ul style="list-style-type: none"> High output torque compared with CSR Short flux path Low MMF requirement High electromagnetic utilization No flux reversal in the stator No mechanical protrusion on the rotor surface 	<ul style="list-style-type: none"> Average torque reduction compared to SSRM with FPW Limited slot area Complex rotor assembly 	<ul style="list-style-type: none"> Aerospace, such as aircraft engines High speed drives, such as fans and gas turbines Automobile drive motor military and household applications
Axial field segmental rotor type	CW [37,38]	<ul style="list-style-type: none"> High output torque compared with CSR Short flux path Low magnetomotive force requirement No flux reversal in the stator No mechanical protrusion on the rotor surface 	<ul style="list-style-type: none"> Complex stator and rotor manufacture Limited slot area Unbalanced axial force resulting large vibration and noise 	<ul style="list-style-type: none"> Low speed high torque application Automobile drive motor household applications
Segmental stator type	CW [48–50,53]	<ul style="list-style-type: none"> High output torque compared with CSR Short flux path Low MMF requirement No flux reversal in the stator High reliability and fault tolerance Low weight 	<ul style="list-style-type: none"> Average torque lower compared to segmental rotor type Complex stator assembly 	<ul style="list-style-type: none"> Low cost high capacity drive application High speed drives household applications, such as blower, fans
Double-stator type	FPW [67,68]	<ul style="list-style-type: none"> High output torque compared with CSR Variable flux math based on the winding conduction mode No flux reversal in the stator High reliability and fault tolerance 	<ul style="list-style-type: none"> Complex structure Manufacture difficult High cost Poor heat dissipation 	<ul style="list-style-type: none"> Low speed high torque application Aerospace Automobile drive motor Not suitable for high-speed drive
Bearingless type	CW [76,77]	<ul style="list-style-type: none"> High output torque compared with traditional BSRM Short flux math No flux reversal in the inner and outer stator Decoupling control between torque and suspension force Steady suspension force 	<ul style="list-style-type: none"> Complex structure Manufacture difficult High cost 	<ul style="list-style-type: none"> High speed drives High precision application Ultra clean application
Hybrid excitation type	FPW [84,88]	<ul style="list-style-type: none"> High output torque compared with CSR High efficiency High power density Low weight Stronger load capacity at low current 	<ul style="list-style-type: none"> Longer end winding in the inner stator Complex structure Manufacture difficult High cost PM is easy to demagnetize 	<ul style="list-style-type: none"> Automobile drive motor High speed drives household applications Not suitable for harsh environment applications

4. Conclusions and Future Directions

The SSRM, emerging as a new structure of the SRM, inherits the advantages of the traditional structure of SRM and improves the performance of the motor. It furthermore has the advantages of shorter flux path, low weight, and reduced core loss. Further improvement in fault tolerance and reliability also increases its applications in electric/hybrid vehicles and aerospace. There are many ontological structures of the SSRM, which are ultimately evolved from the most basic segmental rotor and segmental stator structures. In a novel design of the SRM in which a toothed rotor is replaced with one containing a series

of discrete segments, the segments' rotor achieves isolation between adjacent rotor poles, and the cylindrical rotor structure reduces wind resistance when the motor is running at high speed. The segmental stator achieves magnetic, thermal, and electrical isolation between adjacent phases, which improves core utilization, reduces costs, and improves fault tolerance. Based on the two basic structures, new types of SRMs, such as segmental rotor BSRM, HESSRM, axial segmental SRM, and double-stator SSRM, have gradually evolved. In this paper, we analyze and summarize the existing structural topology design of the SSRM and compare the advantages and disadvantages of various structures and their respective applications in terms of electromagnetism, as Table 1 shows. However, due to the specificity of their structures, there is still a long way to go for large-scale industrial applications. The future research on the SSRM structure is mainly concentrated on the following aspects:

- Expansion of new ontological structure: The higher degree of freedom in the design of the topology of the segmental SRM, currently aiming at permanent magnet-assisted AFSRM, segmental LSRM, and flux switching segmental SRM, combined with the segmental stator, will be an essential direction for the future development of the topological structure;
- Iron loss calculation, vibration noise, and temperature field: Recent studies on the SSRM have focused on electromagnetic properties, but little research has been done on its tower physical fields. Temperature also affects the electromagnetic performance of the motor, and vibration noise is one of the inherent disadvantages of the SSRM. Improving the research gaps of the SSRM and expanding its application area are future research priorities;
- Optimized design of structure with multiple physical fields: At present, many researchers only focus on the optimization of the electromagnetic performance of the SSRM, while in the mechanical aspects, such as vibration, noise, temperature, and other aspects, the related studies are still too few; we should have a comprehensive consideration of each optimization target, which can be combined with some advanced intelligent optimization algorithms for more comprehensive optimization. Then, the motor torque density, efficiency, vibration, noise and other performance indicators could be optimized simultaneously;
- Advanced control technology: all kinds of research are only focusing on the topology of the SSRM, while the research on its control is still very limited. Research on the motor body matching the drive topology and the control strategy are needed to further optimize the performance of the motor and broaden the application field of the SSRM, which is also an important direction for the future development.

Author Contributions: Conceptualization, Z.X.; investigation, T.L.; resources, Z.X. and Y.Z.; data curation, Z.X. and T.L.; writing—original draft preparation, Z.X. and T.L.; writing—review and editing, Z.X., F.Z. and J.-W.A.; visualization, Z.X.; supervision, F.Z., D.-H.L. and J.-W.A.; project administration, Z.X. and F.Z.; funding acquisition, Z.X. and F.Z. All authors have read and agreed to the published version of the manuscript.

Funding: This research was funded by the National Natural Science Foundation of China under Grants 52077141, 52211540392 and 51920105011, Natural Science Foundation of Liaoning Province of China under Grant 2022-MS-269, and Shenyang Young and Middle-Aged Science and Technology Innovation Talent Support Program of China under Grant RC200427.

Data Availability Statement: Not applicable.

Conflicts of Interest: The authors declare no conflict of interest.

Abbreviations

SRM	switched reluctance motor
PMSM	permanent magnet synchronous motor
EVs	electric vehicles
SSRM	segmental switched reluctance motor
PMs	permanent magnets
IM	induction motor
CSRM	conventional switched reluctance motor
BSRM	bearingless switched reluctance motor
SynSRM	synchronous reluctance motor
FPW	full pitch winding
CW	concentrated winding
DTC	direct torque control
DITC	direct instantaneous torque control
ATSMC	adaptive terminal sliding mode control
AFSRM	axial field switched reluctance motors
MMF	magnetic motive force
FRFS-SRM	flux-reversal-free-stator switched reluctance motor
DSSRM	double-stator segmental switched reluctance motor
HESSRM	hybrid excitation segmented switched reluctance motor
LSRM	linear switched reluctance motor

References

- Valdivia, V.; Todd, R.; Bryan, F.J.; Barrado, A.; Lázaro, A.; Forsyth, A.J. Behavioral modeling of a switched reluctance generator for aircraft power systems. *IEEE Trans. Ind. Electron.* **2014**, *61*, 2690–2699. [[CrossRef](#)]
- Yi, F.; Cai, W. Modeling, control, and seamless transition of the bidirectional battery-driven switched reluctance motor/generator drive based on integrated multiport power converter for electric vehicle applications. *IEEE Trans. Power Electron.* **2016**, *31*, 7099–7111.
- Chiba, A.; Kiyota, K.; Hoshi, N.; Takemoto, M.; Ogasawara, S. Development of a rare-earth-free SR motor with high torque density for hybrid vehicles. *IEEE Trans. Energy Convers.* **2015**, *30*, 175–182. [[CrossRef](#)]
- Gan, C.; Wu, J.; Hu, Y.; Yang, S.; Cao, W.; Guerrero, J.M. New integrated multilevel converter for switched reluctance motor drives in plug-in hybrid electric vehicles with flexible energy conversion. *IEEE Trans. Power Electron.* **2017**, *32*, 3754–3766. [[CrossRef](#)]
- Chen, H.; Gu, J. Implementation of the three-phase switched reluctance machine system for motors and generators. *IEEE ASME Trans. Mechatron.* **2010**, *15*, 421–432. [[CrossRef](#)]
- Takemoto, M.; Shimada, K.; Chiba, A. A design and characteristics of switched reluctance type bearingless motors. In Proceedings of the 4th International Symposium on Magnetic Suspension Technology, Gifu, Japan, 30 October–1 November 1997; pp. 49–63.
- Lawrenson, P.J.; Agu, L. A new unexcited synchronous machine. *IEEE Proc.* **1963**, *110*, 1275.
- Morel, L.; Fayard, H.; Vives, F.H.; Abba, G. Study of ultra high speed switched reluctance motor drive. In Proceedings of the IEEE Industry Applications Conference, Rome, Italy, 8–12 October 2000; pp. 87–92.
- Hamdy, R.; Fletcher, J.E.; Williams, B.W.; Finney, S.J. High-speed performance improvements of a two-phase switched reluctance machine utilizing rotor conducting screens. *IEEE Trans. Energy Convers.* **2002**, *17*, 500–506. [[CrossRef](#)]
- Mecrow, B.C.; Finch, J.W.; El-Kharashi, E.A.; Jack, A.G. Switched reluctance motors with segmental rotors. *IEE Proc. Electr. Power Appl.* **2002**, *149*, 245–254. [[CrossRef](#)]
- Mecrow, B.C.; Finch, J.W.; El-Kharashi, E.A.; Jack, A.G. The design of switched reluctance motors with segmental rotors. In Proceedings of the 5th International Conference on Electrical Machines (ICEM), Brugge, Belgium, 25–28 August 2002.
- Mecrow, B.C.; El-Kharashi, E.A.; Finch, J.W.; Jack, A.G. Preliminary performance evaluation of switched reluctance motors with segmental rotors. *IEEE Trans Energy Convers.* **2004**, *19*, 679–686. [[CrossRef](#)]
- Oyama, J.; Higuchi, T.; Abe, T.; Tanaka, K. The fundamental characteristics of novel switched reluctance motor with segment core embedded in aluminum rotor block. In Proceedings of the 8th International Conference on Electrical Machines and Systems, Nanjing, China, 27–29 September 2005; pp. 515–519.
- Oyama, J.; Higuchi, T.; Abe, T.; Tanaka, K. Novel switched reluctance motor with segment core embedded in aluminum rotor block. *Trans. Electr. Eng. Jpn.* **2006**, *126*, 385–390. [[CrossRef](#)]
- Higuchi, T.; Suenaga, K.; Abe, A. Torque ripple reduction of novel segment type Switched reluctance motor by increasing phase number. In Proceedings of the International Conference on Electrical Machines and Systems, Tokyo, Japan, 15–18 November 2009; pp. 1–4.
- Higuchi, T.; Ueda, T.; Abe, T. Torque ripple reduction control of a novel segment type SRM with 2-steps slide rotor. In Proceedings of the International Power Electronics Conference, Sapporo, Japan, 21–24 June 2010; pp. 2175–2180.

17. Matsuo, Y.; Higuchi, T.; Abe, T. Characteristics of a novel segment type switched reluctance motor using grain-oriented electric steel. In Proceedings of the International Conference on Electrical Machines and Systems, Beijing, China, 20–23 August 2011; pp. 1–4.
18. Vattikuti, N.; Rallabandi, V.; Fernandes, B.G. A novel high torque and low weight segmented switched reluctance motor. In Proceedings of the IEEE Power Electronics Specialists Conference, Rhodes, Greece, 15–19 June 2008; pp. 1223–1228.
19. Vandana, R.; Vattikuti, N.; Fernandes, B.G. A novel high power density segmented switched reluctance machine. In Proceedings of the IEEE Industry Applications Society Annual Meeting, Edmonton, AB, Canada, 5–9 October 2008; pp. 1–7.
20. Chen, X.; Wu, J. Calculation of inductances with 3-D FEM for SRM with segmental rotors and fully-pitched windings. In Proceedings of the 17th International Conference on Electrical Machines and Systems, Hangzhou, China, 22–25 October 2014; pp. 1822–1824.
21. Chen, X.; Deng, Z.; Wang, X.; Peng, J.; Li, X. New designs of switched reluctance motors with segmental rotors. In Proceedings of the 5th IET International Conference on Power Electronics, Machines and Drives, Brighton, UK, 19–21 April 2010; pp. 1–6.
22. Mecrow, B.C.; El-Kharashi, E.A.; Finch, J.W.; Jack, A.G. Segmental rotor switched reluctance motors with single-tooth windings. *IEE Proc. Electr. Power Appl.* **2003**, *150*, 591–599. [[CrossRef](#)]
23. Widmer, J.D.; Mecrow, B.C. Optimized segmental rotor switched reluctance machines with a greater number of rotor segments than stator slots. *IEEE Trans. Ind. Appl.* **2013**, *49*, 1491–1498. [[CrossRef](#)]
24. Xu, Z.; Ahn, J. A novel 6/5 segmental rotor type switched reluctance motor: Concept, design and analysis. In Proceedings of the International Conference on Electrical Machines and Systems, Busan, Republic of Korea, 26–29 October 2013; pp. 582–585.
25. Xu, Z.; Jeong, K.; Lee, D.; Ahn, J. Preliminary performance evaluation of a novel 12/8 segmental rotor type SRM. In Proceedings of the 19th International Conference on Electrical Machines and Systems, Chiba, Japan, 13–16 November 2016; pp. 1–5.
26. Xu, Z.; Liu, J.; Kim, M.; Lee, D.; Ahn, J. Characteristics analysis and comparison of conventional and segmental rotor type 12/8 switched reluctance motors. *IEEE Trans. Ind. Appl.* **2019**, *55*, 3129–3137. [[CrossRef](#)]
27. Powell, D.J.; Jewell, G.D.; Calverley, S.D.; Howe, D. Iron loss in a modular rotor switched reluctance machine for the “More-Electric” aero-engine. *IEEE Trans. Magn.* **2005**, *41*, 3934–3936. [[CrossRef](#)]
28. Powell, D.J.; Jewell, G.D.; Howe, D. Rotor topologies for a switched-reluctance machine for the “more-electric” aircraft engine. *IEE Proc. Electr. Power Appl.* **2003**, *150*, 311–318. [[CrossRef](#)]
29. Zhou, Z.; Sun, X.; Chen, L.; Yang, Z.; Li, K.; Zhu, J.; Guo, Y. A segmented rotor type switched reluctance machine for BSGs of hybrid electric vehicles: Concept, design and analysis. In Proceedings of the 20th International Conference on Electrical Machines and Systems, Sydney, Australia, 11–14 August 2017; pp. 1–4.
30. Sun, X.; Zhou, Z.; Chen, L.; Yang, Z.; Han, S. Performance analysis of segmented rotor switched reluctance motors with three types of winding connections for belt-driven starter generators of hybrid electric vehicles. *COMPEL Int. J. Comput. Mathema. Electr. Electron. Eng.* **2018**, *37*, 1258–1270. [[CrossRef](#)]
31. Sun, X.; Zhang, X.; Han, W.; Chen, L.; Xu, X.; Yang, Z. Comparative study of fault-tolerant performance of a segmented rotor SRM and a conventional SRM. *Bull. Pol. Acad. Sci. Tech. Sci.* **2017**, *65*, 375–381. [[CrossRef](#)]
32. Sun, X.; Shen, Y.; Wang, S.; Lei, G.; Yang, Z.; Han, S. Core losses analysis of a novel 16/10 segmented rotor switched reluctance BSG motor for HEVs using nonlinear lumped parameter equivalent circuit model. *IEEE ASME Trans. Mecha.* **2018**, *23*, 747–757. [[CrossRef](#)]
33. Sun, X.; Diao, K.; Lei, G.; Guo, Y.; Zhu, J. Study on segmented-rotor switched reluctance motors with different rotor pole numbers for BSG system of hybrid electric vehicles. *IEEE Trans. Veh. Technol.* **2019**, *68*, 5537–5547. [[CrossRef](#)]
34. Lawrenson, P.J.; Stephenson, J.M.; Blenkinsop, P.T.; Corda, J.; Fulton, N.N. Variable-speed switched reluctance motors. *IEE Proc. Electr. Power Appl.* **1980**, *127*, 253–265. [[CrossRef](#)]
35. Vandana, R.; Fernandes, B.G. Design methodology for high-performance segmented rotor switched reluctance motors. *IEEE Trans. Energy Convers.* **2015**, *30*, 11–21.
36. Sun, X.; Diao, K.; Lei, G.; Guo, Y.; Zhu, J. Real-time HIL emulation for a segmented-rotor switched reluctance motor using a new magnetic equivalent circuit. *IEEE Trans. Power Electron.* **2020**, *35*, 3841–3849. [[CrossRef](#)]
37. Wang, B.; Lee, D.; Ahn, J. A novel axial field SRM with segmental rotor: Concept, design and analysis. In Proceedings of the 2013 Workshop on Power Electronics and Power Quality Applications, Bogota, Colombia, 6–7 July 2013; pp. 1–6.
38. Wang, B.; Lee, D.; Ahn, J. Segmental rotor axial field switched reluctance motor with single teeth winding. In Proceedings of the IEEE 23rd International Symposium on Industrial Electronics, Istanbul, Turkey, 1–4 June 2014; pp. 890–895.
39. Sun, W.; Li, Q.; Sun, L.; Zhu, L.; Li, L. Electromagnetic analysis on novel rotor-segmented axial-field SRM based on dynamic magnetic equivalent circuit. *IEEE Trans. Magn.* **2019**, *55*, 1–5. [[CrossRef](#)]
40. Hall, R.; Jack, A.G.; Mecrow, B.C.; Mitcham, A.J. Design and initial testing of an outer rotating segmented rotor switched reluctance machine for an aero-engine shaft-line-embedded starter/generator. In Proceedings of the IEEE International Conference on Electric Machines and Drives, San Antonio, TX, USA, 15 May 2005; pp. 1870–1877.
41. Vandana, R.; Fernandes, B.G. Segmented switched reluctance motor with novel winding and excitation strategy. In Proceedings of the International Conference on Electrical Machines, Rome, Italy, 6–8 September 2010; pp. 1–4.
42. Nikam, S.P.; Rallabandi, V.; Fernandes, B.G. A high-torque-density permanent-magnet free motor for in-wheel electric vehicle application. *IEEE Trans. Ind. Appl.* **2012**, *48*, 2287–2295. [[CrossRef](#)]

43. Vandana, R.; Nikam, S.; Fernandes, B.G. High torque polyphase segmented switched reluctance motor with novel excitation strategy. *IET Electr. Power Appl.* **2012**, *6*, 375. [[CrossRef](#)]
44. Zhang, H. Design and Control of a Novel 12/8 Segmented Rotor Type SRM. Ph.D. Thesis, Shenyang University of Technology, Shenyang, China, 2015.
45. Chen, L.; Wang, H.; Sun, X.; Cai, Y.; Li, K.; Diao, K.; Wu, J. Development of a digital control system for a belt-driven starter generator segmented switched reluctance motor for hybrid electric vehicles. *Proc. Inst. Mech. Eng. Part I J. Syst. Control Eng.* **2020**, *234*, 975–984. [[CrossRef](#)]
46. Zhou, Z. A Segmented-Rotor Switched Reluctance Motor and Its Direct Torque Control for the BSG Used in Mild Hybrid Electric Vehicles. Ph.D. Thesis, Jiangsu University, Zhenjiang, China, 2019.
47. Sun, X.; Feng, L.; Diao, K.; Yang, Z. An improved direct instantaneous torque control based on adaptive terminal sliding mode for a segmented-rotor SRM. *IEEE Trans. Ind. Electron.* **2021**, *68*, 10569–10579. [[CrossRef](#)]
48. Lee, C.; Krishnan, R.; Lobo, N.S. Novel two-phase switched reluctance machine using common-pole E-core structure: Concept, analysis, and experimental verification. *IEEE Trans. Ind. Appl.* **2009**, *45*, 703–711. [[CrossRef](#)]
49. Tanujaya, M.; Lee, D.; Ahn, J. Characteristic analysis of a novel 6/5 c-core type three-phase switched reluctance motor. In Proceedings of the International Conference on Electrical Machines and Systems, Beijing, China, 20–23 August 2011; pp. 1–6.
50. Trung Hieu, P.; Lee, D.; Ahn, J. Design and control of a high speed segmental stator 4/3 switched reluctance motor. In Proceedings of the IEEE Transportation Electrification Conference and Expo, Asia-Pacific, Busan, Korea, 1–4 June 2016; pp. 767–772.
51. Lee, D.; Trung Hieu, P.; Ann, J. Design and operation characteristics of four-two pole high-speed SRM for torque ripple reduction. *IEEE Trans. Ind. Electron.* **2013**, *60*, 3637–3643. [[CrossRef](#)]
52. Lobo, N.S.; Swint, E.; Krishnan, R. M-phase N-segment flux-reversal-free stator switched reluctance machines. In Proceedings of the IEEE Industry Applications Society Annual Meeting, Edmonton, Canada, 5–9 October 2008; pp. 1–8.
53. Shang-Hsun, M.; Mi-Ching, T. A novel switched reluctance motor with C-core stators. *IEEE Trans. Magn.* **2005**, *41*, 4413–4420. [[CrossRef](#)]
54. Ding, W.; Hu, Y.; Wu, L. Characteristics comparison of conventional and modular E-core stator with segmental rotor switched reluctance motors. In Proceedings of the 17th International Conference on Electrical Machines and Systems, Hangzhou, China, 22–25 October 2014; pp. 1797–1801.
55. Ding, W.; Hu, Y.; Wu, L.; Yang, S. Comprehensive research of modular E-core stator hybrid-flux switched reluctance motors with segmented and non-segmented rotors. *IEEE Trans. Energy Convers.* **2017**, *32*, 382–393. [[CrossRef](#)]
56. Ding, W.; Ying, G.; Liu, L.; Lou, J. Magnetic circuit model and finite-element analysis of a modular switched reluctance machine with E-core stators and multi-layer common rotors. *IET Electr. Power Appl.* **2014**, *8*, 296–309. [[CrossRef](#)]
57. Ding, W.; Hu, Y.; Fu, H.; Chen, Q. Analysis of novel segmented E-shaped stator switched reluctance machines with segmental and conventional rotor topologies. In Proceedings of the 11th International Conference on Ecological Vehicles and Renewable Energies, Monte Carlo, Monaco, 6–8 April 2016; pp. 1–8.
58. Ding, W.; Hu, Y.; Wu, L. Analysis and development of novel three-phase hybrid magnetic paths switched reluctance motors using modular and segmental structures for EV applications. *IEEE/ASME Trans. Mechatronics.* **2015**, *20*, 2437–2451. [[CrossRef](#)]
59. Szabo, L.; Ruba, M. Segmental stator switched reluctance machine for safety-critical applications. *IEEE Trans. Ind. Appl.* **2012**, *48*, 2223–2229. [[CrossRef](#)]
60. Ruba, M.; Viorel, I.A.; Szabo, L. Modular stator switched reluctance motor for fault tolerant drive systems. *IET Electr. Power Appl.* **2013**, *7*, 159–169. [[CrossRef](#)]
61. Asgar, M.; Afjei, E.; Torkaman, H. A new strategy for design and analysis of a double-stator switched reluctance motor: Electromagnetics, FEM, and experiment. *IEEE Trans. Magn.* **2015**, *51*, 1–8. [[CrossRef](#)]
62. Bostanci, E.; Gu, L.; Cosoroaba, E.; Moallem, M.; Fahimi, B. Performance improvement and comparison of concentrated winding segmental rotor and double stator switched reluctance machines. In Proceedings of the IEEE Conference on Electromagnetic Field Computation, Miami, FL, USA, 13–16 November 2016; p. 1.
63. Abbasian, M.; Moallem, M.; Fahimi, B. Double-stator switched reluctance machines (DSSRM): Fundamentals and magnetic force analysis. *IEEE Trans. Energy Convers.* **2010**, *25*, 589–597. [[CrossRef](#)]
64. Isfahani, A.H.; Fahimi, B. Comparison of mechanical vibration between a double-stator switched reluctance machine and a conventional switched reluctance machine. *IEEE Trans. Magn.* **2014**, *50*, 293–296. [[CrossRef](#)]
65. Cosoroaba, E.; Wang, W.; Fahimi, B. Comparative study of two winding configurations for a double stator switched reluctance machine. In Proceedings of the 2014 International Conference on Electrical Machines, Berlin, Germany, 2–5 September 2014; pp. 1013–1017.
66. Kondelaji, M.A.J.; Mirsalim, M. Segmented-rotor modular switched reluctance motor with high torque and low torque ripple. *IEEE Trans. Transp. Electrification.* **2020**, *6*, 62–72. [[CrossRef](#)]
67. Cheng, H.; Liao, S.; Yan, W. Development and Performance Analysis of Segmented-Double-Stator Switched Reluctance Machine. *IEEE Trans. Ind. Electron.* **2022**, *69*, 1298–1309. [[CrossRef](#)]
68. Yan, W.; Cheng, H.; Liao, S.; Liu, Y. Design of a low-ripple double-modular-stator switched reluctance machine for electric vehicle applications. *IEEE Trans. Transp. Electrification.* **2021**, *7*, 1349–1358. [[CrossRef](#)]

69. Yan, W.; Chen, H.; Ma, X.; Orabi, M.; Lv, Z. A low ripple double modular-stator switched reluctance machine for electric vehicles applications. In Proceedings of the IEEE International Conference on Applied Superconductivity and Electromagnetic Devices, Tianjin, China, 16–18 October 2020; pp. 1–2.
70. Sun, Q.; Wu, J.; Gan, C.; Shi, C.; Guo, J. DSSRM design with multiple pole arcs optimization for high torque and low torque ripple applications. *IEEE Access* **2018**, *6*, 27166–27175. [[CrossRef](#)]
71. Lin, C.; Wang, W.; Fahimi, B. Optimal design of double stator switched reluctance machine (DSSRM). In Proceedings of the IEEE International Symposium on Industrial Electronics, Hangzhou, China, 28–31 May 2012; pp. 719–724.
72. Wang, W.; Luo, M.; Cosoroaba, E.; Fahimi, B.; Kiani, M. Rotor shape investigation and optimization of double stator switched reluctance machine. *IEEE Trans. Magn.* **2015**, *51*, 1–4. [[CrossRef](#)]
73. Tavakkoli, M.A.; Moallem, M. Torque ripple mitigation of double stator switched reluctance motor (DSSRM) using a novel rotor shape optimization. In Proceedings of the IEEE Energy Conversion Congress and Exposition, Raleigh, NC, USA, 15–20 September 2012; pp. 848–852.
74. Peng, W.; Xu, Z.; Lee, D.; Ann, J. Control of radial force in double stator type bearingless switched reluctance motor. *J. Electr. Eng. Technol.* **2013**, *8*, 766–772. [[CrossRef](#)]
75. Huang, Y.; Huang, F.; Yuan, Y.; Yang, F.; Xie, K. Design and analysis of a novel bearingless segmented switched reluctance motor. *IEEE Access* **2019**, *7*, 94342–94349. [[CrossRef](#)]
76. Fan, Z.; Xu, Z.; Wang, H.; Zhang, F. Characteristics analysis of a novel 12/8 double stator bearingless switched reluctance motor. In Proceedings of the 24th International Conference on Electrical Machines and Systems, Gyeongju, Republic of Korea, 31 October–3 November 2021; pp. 333–338.
77. Xu, Z.; Zhou, Z.; Fan, Z.; Qi, Y.; Zhang, F. Characteristics analysis and comparison of conventional and segmental rotor type 12/8 double stator bearingless switched reluctance motors. In Proceedings of the Joint MMM-Intermag Conference, New Orleans, LA, USA, 10–14 January 2022; pp. 1–5.
78. Hasegawa, Y.; Nakamura, K.; Ichinokura, O. Basic consideration of switched reluctance motor with auxiliary windings and permanent magnets. In Proceedings of the IEEE International Conference on Electrical Machines, Marseille, France, 2–5 September 2012; pp. 92–97.
79. Kenji, N.; Kohei, M.; Osam, I. Characteristics of a novel switched reluctance motor having permanent magnets between the stator pole-tips. In Proceedings of the European Conference on Power Electronics and Applications, Aalborg, Denmark, 2–5 September 2007; pp. 1–5.
80. Hwang, H.; Bae, S.; Lee, C. Analysis and design of a hybrid rare-earth-free permanent magnet reluctance machine by frozen permeability method. *IEEE Trans. Magn.* **2016**, *52*, 8106304. [[CrossRef](#)]
81. Ullah, S.; McDonald, S.P.; Martin, R.; Atkinson, G.J. A permanent magnet assisted switched reluctance machine for more electric aircraft. In Proceedings of the International Conference on Electrical Machines, Lausanne, Switzerland, 4–7 September 2016; pp. 79–85.
82. Pang, M.; Wang, H.; Zhou, G.; Li, F.; Wei, X.; Zhang, M. Design and analysis of a two-phase permanent-magnet-assisted switched reluctance motor. In Proceedings of the 21st International Conference on Electrical Machines and Systems, Jeju, Republic of Korea, 7–10 October 2018; pp. 1956–1961.
83. Zhu, J.; Cheng, K.W.E.; Xue, X. Design and analysis of a new enhanced torque hybrid switched reluctance motor. *IEEE Trans. Energy Convers.* **2018**, *33*, 1965–1977. [[CrossRef](#)]
84. Ding, W.; Yang, S.; Hu, Y.; Li, S.; Wang, T.; Yin, Z. Design Consideration and Evaluation of a 12/8 High-Torque Modular-Stator Hybrid Excitation Switched Reluctance Machine for EV Applications. *IEEE Trans. Ind. Electron.* **2017**, *64*, 9221–9232. [[CrossRef](#)]
85. Andrada, P.; Blanqué, B.; Martínez, E.; Torrent, M. A novel type of hybrid reluctance motor drive. *IEEE Trans. Ind. Electron.* **2014**, *8*, 4337–4345. [[CrossRef](#)]
86. Ding, W.; Fu, H.; Hu, Y. Characteristics assessment and comparative study of a segmented-stator permanent-magnet hybrid-excitation SRM drive with high-torque capability. *IEEE Trans. Power Electron.* **2018**, *33*, 482–500. [[CrossRef](#)]
87. Tai, W.; Tsai, M.; Gaing, Z.; Huang, P.; Hsu, Y. Novel stator design of double salient permanent magnet motor. *IEEE Trans. Magn.* **2014**, *50*, 1–4. [[CrossRef](#)]
88. Kondelaji, M.A.J.; Mirsalim, M. Double-stator PM-assisted modular variable reluctance motor for EV applications. In Proceedings of the 9th Annual Power Electronics, Drives Systems and Technologies Conference, Tehran, Iran, 13–15 February 2018; pp. 236–240.
89. Ganji, B.; Askari, M.H. Different topologies for linear switched reluctance motor with segmental translator. In Proceedings of the 24th Iranian Conference on Electrical Engineering, Shiraz, Iran, 10–12 May 2016; pp. 874–878.
90. Yi, X.; Zhu, C.; Huang, C.; Wang, D.; Wang, X. Design Optimization of Linear Switched Reluctance Motor with Segmental Mover. In Proceedings of the 13th International Symposium on Linear Drives for Industry Applications, Wuhan, China, 1–3 July 2021; pp. 1–6.
91. Wang, D.; Du, X.; Zhang, D.; Wang, X. Design, optimization, and prototyping of segmental-type linear switched-reluctance motor with a toroidally wound mover for vertical propulsion application. *IEEE Trans. Ind. Electron.* **2018**, *65*, 1865–1874. [[CrossRef](#)]